Sulfur dioxide in the Venus atmosphere: I. Vertical distribution and variability

Ann Carine Vandaele, Oleg Korablev, Denis Belyaev, Sarah Chamberlain, Daria Evdokimova, Thérèse Encrenaz, Larry Esposito, Kandis Lea Jessup, Franck Lefèvre, Sanjay Limaye, et al.

Highlights

- Large SO_2 and SO variability in the Venus atmosphere is observed
- SO_2 abundance in the Venus atmosphere shows an inversion layer located around 70-75 km
- GCM modelling indicates that dynamics may play a role in generating the inversion

Sulfur Dioxide in the Venus Atmosphere: I. Vertical distribution and variability

A.C. Vandaele[a,†], O. Korablev[b,c], D. Belyaev[b], S. Chamberlain[a], D. Evdokimova[b], Th. Encrenaz[d], L. Esposito[e], K.L. Jessup[f,g], F. Lefèvre[h], S. Limaye[i], A. Mahieux[a,j], E. Marcq[k], F.P. Mills[g,l], F. Montmessin[k], C.D. Parkinson[m], S. Robert[a], T. Roman[n], B. Sandor[n], A. Stolzenbach[h], C. Wilson[o], V. Wilquet[a]

[a] Planetary Aeronomy, Royal Belgian Institute for Space Aeronomy, Brussels, Belgium

[b] Space Research Institute (IKI), Moscow 117997, Russia

[c] Moscow Institute of Physics and Technology (MIPT), Dolgoprudny 141700, Russia

[d] Observatoire Paris-Site de Meudon (LESIA), Meudon, France

[e] LASP - University of Colorado, Boulder, CO 80303-7814, USA

[f] Department of Space Science, Southwest Research Institute, Boulder, CO 80302, USA

[g] Fenner School of Environment and Society, Australian National University, ACT, Australia

[h] LATMOS, CNRS, Université Pierre et Marie Curie, Paris, France

[i] University of Wisconsin-Madison, Madison, WI 53706, USA

[j] Fonds National de la Recherche Scientifique, rue d'Egmond 5, 1000 Brussels, Belgium

[k] LATMOS, CNRS, Université de Versailles Saint-Quentin-en-Yvelines, Guyancourt, France

[l] Space Science Institute, Boulder, CO, 80303, USA

[m] University of Michigan, Ann Arbor, MI, 48109 USA

[n] Space Telescope Science Institute, Baltimore, MD 21218, USA

[o] University of Oxford, UK

[†] to whom correspondence should be sent (a-c.vandaele@aeronomie.be - Planetary Aeronomy, Royal Belgian Institute for Space Aeronomy, Avenue Circulaire 3, 1180 Brussels, Belgium – Tel: +32(0)2-373.03.67)

Abstract

Recent observations of sulfur containing species (SO_2, SO, OCS, and H_2SO_4) in Venus' mesosphere have generated controversy and great interest in the scientific community. These observations revealed unexpected spatial patterns and spatial/temporal variability that have not been satisfactorily explained by models. Sulfur oxide chemistry on Venus is closely linked to the global-scale cloud and haze layers, which are composed primarily of concentrated sulfuric acid. Sulfur oxide observations provide therefore important insight into the on-going chemical evolution of Venus' atmosphere, atmospheric dynamics, and possible volcanism.

This paper is the first of a series of two investigating the SO_2 and SO variability in the Venus atmosphere. This first part of the study will focus on the vertical distribution of SO_2, considering mostly observations performed by instruments and techniques providing accurate vertical information. This comprises instruments in space (SPICAV/SOIR suite on board Venus Express) and Earth-based instruments (JCMT). The most noticeable feature of the vertical profile of the SO_2 abundance in the Venus atmosphere is the presence of an inversion layer located at about 70-75 km, with VMRs increasing above. The observations presented in this compilation indicate that at least one other significant sulfur reservoir (in addition to SO_2 and SO) must be present throughout the 70-100 km altitude region to explain the inversion in the SO_2 vertical profile. No photochemical model has an explanation for this behaviour. GCM modelling indicates that dynamics may play an important role in generating an inflection point at 75 km altitude but does not provide a definitive explanation of the source of the inflection at all local times or latitudes

The current study has been carried out within the frame of the International Space Science Institute (ISSI) International Team entitled 'SO_2 variability in the Venus atmosphere'.

Keywords

Atmospheric model; reference atmosphere; Venus; sulfur cycle

1 Introduction

Sulfur dioxide, SO_2, is a key element of the sulfur cycle on Venus. It was detected in the Venus atmosphere, above, within and below the clouds, very early in the history of Venus exploration, using Earth-based, space-borne and in situ instrumentation. The recent European Venus Express (VEx) mission ushered a renewed interest in Venus and its complex photochemistry and dynamics, in which the sulfur cycle plays a predominant role. Table 1 summarizes the observations of SO_2 carried out in the 'pre-VEx' era, along with observations performed with VEx instruments and contemporary measurements from Earth or with the Hubble Space Telescope.

SO_2 was first detected in the Venusian upper atmosphere from Earth-based ultraviolet observations with a mixing ratio 0.02–0.5 ppm at the UV cloud top [1]. Space-based identifications of SO_2 UV absorption followed soon with the International Ultraviolet Explorer (IUE) [2] and with *Pioneer Venus Orbiter* (PVO) Ultraviolet Spectrometer (UVS) [3]. The PVO/UVS observations showed a steady decline of the UV cloud top (~ 40 mbar, 68 km) SO_2 content from 100 ppb down to 10 ppb about 10 years later [4]. The decline of the SO_2 amount was rather fast over the first year, and much slower later on. This behaviour was initially interpreted as evidence of a massive "injection of SO_2 into the Venus middle atmosphere by a volcanic explosion" [4]. This steep decline of the SO_2 abundance was also confirmed by IUE observations, which showed a decrease of the abundance from 380±70 ppb in 1979 down to 50±20 ppb in 1988 [5]. Rocket observations carried out in the UV spectral range reported SO_2 abundance of 80±40 ppb and 120±60 ppb for 2 launches performed in 1988 and 1991 respectively [6, 7]. In 1995 a first measurement from the Hubble Space Telescope was performed and yielded a value of 20±10 ppb [8] also indicating a decrease in the SO_2 abundance with time. SO_2 abundance was also monitored with the Fourier spectrometer on board Venera 15 orbiter in 1983. An initial analysis [9] reported an abundance of 2 ppm at an altitude of 60-62 km, with no apparent latitudinal variation. However, later analysis of a more consistent dataset provided new insights on the latitudinal distribution of SO_2 [10]. At the 40 mbar level (69 km), the SO_2 mixing ratio was a few tens of ppb at low latitudes (below 45°), 1-10 ppb in the cold collar region, and 100-200 ppb near the poles. Very large values up to 1000 ppb were observed locally. The same analysis provided similar results at the 150 mbar level (62 km): 0.3-0.5 ppm at low latitudes and 1-2 ppm in polar regions. The two altitude levels were selected to perform a straightforward comparison with the UV observations of PVO/UVS, IUE and the rockets.

Below the clouds, sulfur dioxide was measured in situ by *Venera* and *Pioneer Venus* probes, and by ground based observations in the near-infrared transparency windows (see Table 1 and Figure 1). In the late 1970s the Pioneer Venus Gas Chromatograph (GC) measured abundances of 185±43 ppm at an altitude of 22 km, as well as a lower limit of 176 ppm at 42 km and a higher limit of 600 ppm at 52 km [11, 12]. Such elevated levels were later confirmed by the GC on Venera 12 [13] and the mass spectrometer measurement of the Pioneer Venus probe [14]. Results from the ISAV ultraviolet spectrometers on board the

VEGA 1 and 2 probes were analysed in detail in Bertaux et al. [15]. Both probes provided SO_2 profiles from the cloud top down to the surface: ISAV1 showed a double peak structure at 51.5 and 42.5 km (150 and 125 ppm SO_2 respectively), while ISAV2 had a one peak profile (210 ppm at 43 km). Below 40 km both profiles exhibited the same decrease of SO_2 with decreasing altitude. In the 1990s ground-based observation in the IR allowed the determination of the SO_2 abundance below the clouds: Bézard et al. [16] found a value of 130±40 ppm in the 35-45 km region and Pollack et al. [17] reported the value of 180±70 ppm at an altitude of 42 km. Both are in agreement with the 1985 Vega profiles. Microwave observations are also sensitive to the SO_2 absorption although their results strongly depend on the assumption made on the temperature profile. Such observations suggested low SO_2 mixing ratio below the clouds with values lower than 100 ppm at low latitude and lower than 50 ppm in polar regions [18, 19]. So far, the number of the available measurements and their accuracy did not allow the detection of any variations in SO_2 below the clouds. However, Arney et al. [20], using ground-based spectra in the 2.3 μm window, might have detected a hemispheric dichotomy with slightly more SO_2 in the northern hemisphere, although the difference lies within the retrievals error.

It has been proposed that VEGA SO_2 profiles are decreasing further towards the surface, finally reaching thermochemical equilibrium. Assuming the VEGA1 value of 25 ppm, the thermochemical lifetime of SO_2 is 320000 years [21]. If the SO_2 were not replenished the sulfuric acid, clouds would eventually disappear over geological timescales.

Detailed thermochemical modelling indicates that volcanic outgassing is the most probable primary source of sulfur dioxide in Venus' lower atmosphere [22]. This understanding is supported by recent VEx observations of the surface thermal emission which strongly suggest recent or current volcanic activity [23, 24]. The exchange of SO_2 from the lower to the upper atmosphere is not fully understood, but undoubtedly involves convective transport, presumably in conjunction with Hadley cell circulation. Secular variation of this circulation may alter the SO_2 supply from the lower atmosphere provoking the long-term trends of its abundance above clouds mentioned above. Photochemical oxidation efficiently removes SO_2 from Venus' upper atmosphere leading to the formation of the sulfuric acid droplets making up the clouds and haze enshrouding the planet. As a result the SO_2 abundance above the clouds drops to ppb levels while the SO_2 located below the cloud layer is effectively sequestered from photochemical reactions.

The work presented in this series of two papers is the result of discussions and inter-comparison exercises completed by an International Science Team formed through the International Space Science Institute (ISSI). ISSI sponsored three distinct teams devoted to the study of Venus' atmosphere during 2013-2015. These teams tackled three aspects of the Venus atmosphere that are still not fully understood: i) the structure of the atmosphere (temperature variations with altitude and latitude, and the dynamics related to these variations), ii) the formation and structure of the clouds and iii) the presence of sulfur bearing compounds in the atmosphere, with an emphasis on SO_2 variability. These three topics are of

course intimately entwined and correlated and cannot be investigated independently. As a first step in understanding these relationships, we report lessons learned by the SO_2 variability team regarding the vertical, horizontal, and temporal distribution of SO_2 and its role in maintaining Venus' sulfur chemistry cycle.

This paper is composed of two parts dealing with different aspects of the SO_2 variability within the Venus atmosphere, i.e. vertical, horizontal, and temporal distributions. The focus has been set on recent measurements carried out from Earth or from space-borne instruments. This includes instruments on board Venus Express, such as SPICAV/SOIR and VIRTIS, but also on the Hubble Space Telescope (STIS). These instruments, while providing complementary information, probe the atmosphere differently in terms of the air masses sounded, observational geometry (nadir, limb), and/or the retrieved atmospheric quantities (such as local vs. integrated densities, or density vs. VMR), etc. For this reason the SO_2 variability discussions are segregated into a two-paper series. In part I, we will focus on observations from which information on the vertical distribution can be inferred. This mainly concern SPICAV/SOIR observations performed in solar and stellar occultation, as well as ground-based measurements carried out in the sub-mm range (JCMT). We also use photochemical models to help the interpretation of the observed vertical profiles, as well as results from the VIRTIS, HST, ALMA and TEXES instruments, which tend to probe very specific altitude regions. The part II, the SO_2 spatial (horizontal) and temporal variability is discussed. These later discussions rely on information gathered by mapping instruments, such as SPICAV/UV nadir, HST and ground-based IR (TEXES) and sub-mm (ALMA) instruments.

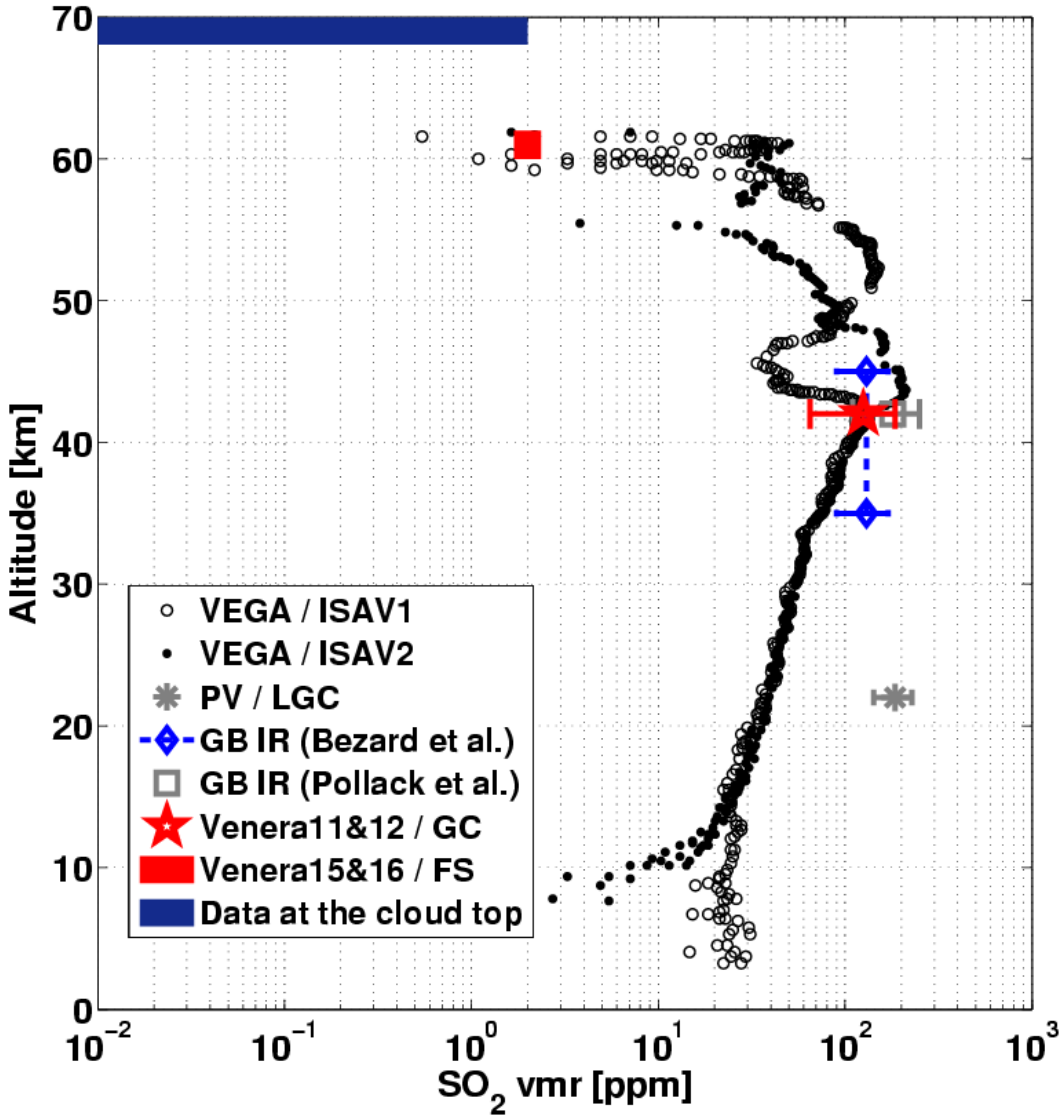

Figure 1: Measurements of SO_2 abundance (expressed in VMR, volume mixing ratio) in the pre-VEx era. Data at Venus' UV cloud top are a summary from different experiments (see Table 1).

Table 1: Summary of SO_2 past observations (pre-VEx era).

Instrument/Mission	**SO_2 VMR**	**Altitude**	**Latitude**	**Scale height (km)**	**Year of observation**	**Ref**
GB UV	20-500 ppb	> 70 km			1977	[1]
PVO/UVS	$1.0x10^{17}$ cm^{-2} column density	> 70 km	-		1978	[3]
PVO/UVS	100 ppb	69 km (40 mbar)	-	1	1978	[25]
PVO/UVS	Reanalysis of UVS/PV 100 ppb (1978) 10 ppb (1986)	69 km (40 mbar)		1.5-2.5 (low Lat) 1 (high Lat)	1978-1986 Decline wrt to 1978	[4]
IUE	100-800 ppb	3-26 mbar			1979	[2]
IUE	50±20 ppb 380±70 ppb*	Cloud top		3±1	1987-1988 1979	[5]
Rockets	60±30 ppb 300±150 ppb 80±40 ppb 120±60 ppb	UV cloud top	< 30° 50S Average Average	3-4 (<30°) 2 (50S)	1988 1991	[6, 7]
HST	20±10 ppb	UV cloud top (40 mbar)		2	1995	[8]
Venera 15 (FS)	2 ppm	60-62 km	Lat independent	1.5	1983	[9]
Venera 15 (FS)	0.1-1 ppb 1-10 ppb 100-200 ppb	69 km (40 mbar)	< 45° Cold collar Near polar	1.5-2.5 (low Lat) 3-5 (high Lat)	1983	[10]

	(up to 1000 ppb) 0.3-0.5 ppm 1-2 ppm		< 45° polar			
PV/LGC	185±43 ppm > 176 ppm < 600 ppm	22 km 42 km 52 km			1978	[11, 12]
Venera 11 & 12 (GC)	130±60 ppm	< 42 km			1978	[13]
PV/MS	< 500 ppm	< 50 km			1978	[14]
VEGA 1 & 2	 ISAV1 /ISAV2 150 / 65 ppm 125 /140 ppm 38 / 38 ppm 25 / 20 ppm	2 Profiles on 10-60 km 52 km 42 km 22 km 12 km		7.5 N (ISAV1) 8.5 S (ISAV2)	1985	[15]
GB IR	180±70 ppm	42 km			1989, 1991	[17]
GB IR	130±40 ppm	35-45 km			1989, 1991	[16]
GB MW	≤ 50 ppm	Below lower cloud			1996, 1999	[18]
GB MW	≤ 50 ppm ≤ 100 ppm	37-45 km	Polar regions Low Lat		1996	[19]

*Revised value of [2]

GC: Gas Chromatograph – UVS: UltraViolet Spectrometer – PVO: Pioneer Venus Orbiter – PV: Pioneer Venus – GB: Ground-based – HST: Hubble Space Telescope – MS: Mass spectrometer – IUE: International Ultraviolet Experiment – LGC: Large Gas Chromatograph – FS: Fourier Spectrometer – IR: InfraRed – MW: MicroWave – VMR: Volume Mixing Ratio

2 SO_2 Observations in the VEx era

In the present study we will focus on recent SO_2 and SO (collectively, SO_x) observations , i.e. observations concurrent with the those carried out by the instruments on board *Venus Express*.

The SPICAV/SOIR (SPectroscopy for Investigation and Characterizations of Atmosphere of Venus/Solar Occultation in the IR) spectrometers' suite [26] on board VEx measured the vertical SO_2 abundance profile at the terminator at 70-100 km based on absorption bands located at 190-220 nm and 270-300 nm (using SPICAV UV [27]) and at 70-90 km altitude, using the absorption at ~4 μm (using SOIR [28, 29]). Additionally, the vertical SO gas profile was extracted from SPICAV UV occultation observations using unresolved SO absorption bands located also in the 190-220 nm spectral range. The occultation observations, stellar and solar, were obtained at multiple latitudes throughout the VEx mission, thereby documenting the latitudinal and temporal variability in the SO_x vertical profiles. Together, SPICAV UV and SOIR occultation observations provided the vertical mesospheric distribution of SO_2 mixing ratio from 70 to 100 km at a high altitude resolution nominally in the range of 0.5-20 km, with an average of 3 km. On-board VEx, the VIRTIS spectrometer probed SO_2 below the clouds measuring the gas absorption in the spectral window at ~2.35 μm corresponding to altitudes of 30-40 km [30].

SO_2 was also observed using ground based telescopes and the Hubble Space Telescope (HST). Hubble's Space Telescope Imaging Spectrograph (STIS) observed Venus using the same SO and SO_2 absorption bands as SPICAV UV (190-220 nm) but with better spectral resolution: $\Delta\lambda$~0.3 nm versus 1.5 nm [31]. These observations mapped the 70-80 km SO_x distribution between morning terminator and subsolar point at a spatial resolution of 150±25 km. Another SO_2 mapping at 60-80 km came from thermal IR spectroscopy (~7.5 μm) made by the ground-based IRTF/TEXES (Infrared Telescope Facility/Texas Echelon-Cross-Echelle Spectrograph) instrument [32]. Microwave observations using the ground-based James Clerk Maxwell Telescope (JCMT) were performed over the 2004-2008 period [33], and provided average values on the Venus disk for SO_2 and SO mixing ratios at altitude level ~85-100 km on both day and night sides. Submillimetre measurements of SO and SO_2 were also performed using the ground-based network of antennas ALMA (Atacama Large Millimeter/Submillimeter Array) in November 2011 [34]. There is also a single observation of SO_2 content made from the IRTF by the CSHELL (Cryogenic Echelle) spectrograph at 4.04 μm in June 2009 [35]. SPICAV also observed SO_2 thanks to its absorption bands near 210 and 280 nm in the backscattered UV sunlight [36, 37]. But the relatively low spectral resolution of SPICAV-UV prevented the independent retrieval of SO, assumed tied to 10% of SO_2.

All observations in this era have shown high variability of SO_2 content in time and in space above the clouds: 20-400 ppbv at the cloud top, 10-200 ppbv above 85 km. Table 2 presents a summary of all the experiments considered in this study. Figure 2 and Figure 3 summarize the

statistics of the sounded altitudes versus local solar time and latitude on Venus. These Figures clearly show that observations are missing at high latitudes (above 80°) and are quasi non-existent below the clouds.

Table 2: Summary of the observations considered in this study. Ranges of observed SO_2 and SO VMRs are indicated for each instrument as well as the altitudes range sounded.

Observation	**Resolving power, λ/Δλ**	**Altitude range, km**	**SO_2 VMR, ppbv**	**SO VMR, ppbv**	**Concerns/notes**	**ref**
TEXES 7.5 µm	80 000	60-85	75-125	no	High variability	[32]
TEXES 19 µm	80 000	57-85	75-125	no	High variability	[38]
ALMA 346.6 GHz	10^6	70-100	8-16 [z>88km] 0 [z<88km]	8±2 [z>88 km]	High variability	[34]
CSHELL 4 µm	40 000	72	200-600	--------	SO_2 and OCS	[35]
SPICAV UV nadir 190-300 nm	150-200	70-80	20-800	assumed $0.1\times SO_2$	VMR decreases from 2007 to 2012 (peak suspected in 2007)	[37]
UV HST 190-300 nm	700-1000	70-80	6-200 above z=75 km;	1-15	Dayside and near terminator values (i.e. SZA = 15-75°) derived from the HST data obtained between 30N and 35S latitude region, for SO_2 and SO gas; VMR derived assuming VIRA CO_2 profile, 0.965 CO_2 abundance	[31]
SOIR 4 µm	20 000	66-80	20-500	--------	Terminator; Mostly polar coverage	[27]
		80-90	10-200	--------	Terminator – all latitudes; Coincide with SPICAV-UV assuming no SO	[29]
JCMT 346.6 GHz	10^6-10^7	70-100 (84)	0-70 [z>85 km] 0 [z<83 km]	0-30	Time and diurnally variable	[33]
SPICAV UV occultations 190-300 nm	150-200	85-100	80-100 on avg, Variable up to 500	20-200	Depends on SO retrieval - Total amount of SO_x is 10-100 times higher than expected from µwave	[27]

VIRTIS, 2.4 µm	2000	30-40	130±50 ppm	--------	Spectral resolution is not enough to clarify variations with latitude and time [30]

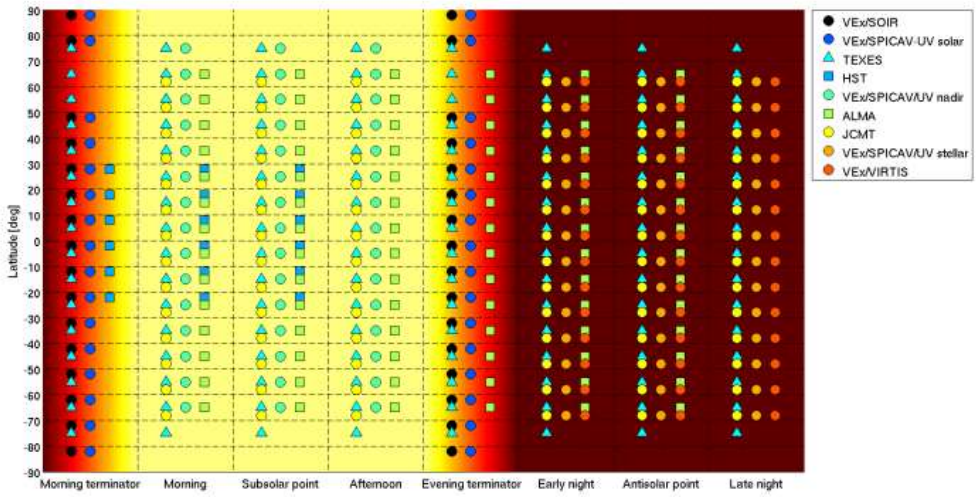

Figure 2: Summary of local solar times and Latitudes sounded by the different instruments.

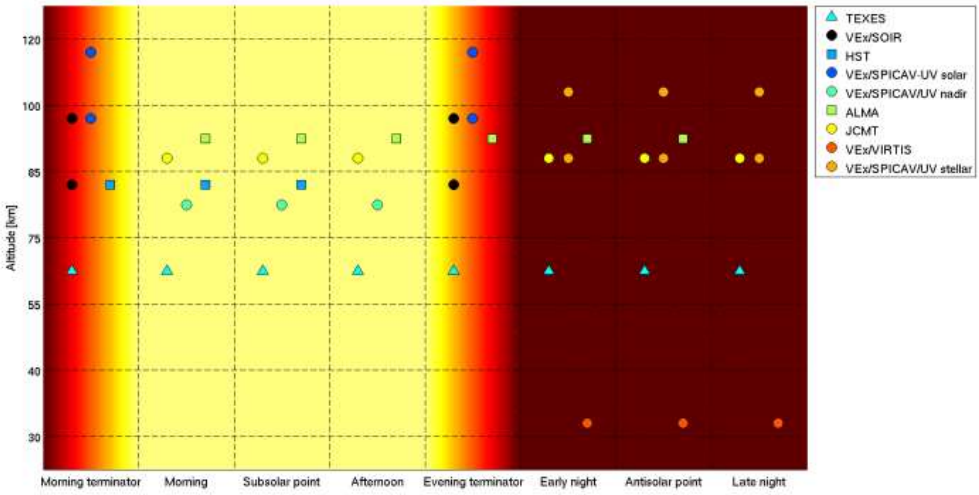

Figure 3: Summary of altitude coverage encountered (independent of observed latitude) vs local solar time.

3 Observations of the vertical distribution of SO and SO_2

One method to acquire accurate information on the vertical profile of any atmospheric species is to scan vertically through the atmosphere measuring absorption or emission spectra with an instrument in orbit around the planet. Several geometries are possible: solar and stellar occultation using the Sun as a source of radiation, or limb scanning sensitive to the emission originating from the sounded layers and/or the solar scattered light. The SPICAV/SOIR on VEx performed routinely solar and stellar observations and provided a huge amount of data allowing the characterization of this rather unknown region from the top of the cloud deck up to 170 km altitude. In some cases, ground-based observations are also sensitive to the vertical profiles of the target species. Sub-millimeter observations are such a technique. In the following, we describe in more details, the instruments and their respective data sets considered for the investigation of the vertical distribution of SO and SO_2 in the Venus atmosphere.

3.1 SOIR

The SOIR (Solar Occultation in the InfraRed) instrument [39] on board the ESA *Venus Express* used the solar occultation technique to sound the mesosphere and the lower thermosphere of the Venus atmosphere. It was sensitive in the 2.3 to 4.4 µm region (2257 to 4430 cm^{-1}) and used an echelle grating at high diffraction orders (101 to 194) associated with an Acousto-optic tuneable filter (AOTF) to select the spectral range to be recorded [40]. The spectral resolution of the instrument was also high and order dependent, ranging from 0.11 cm^{-1} to 0.21 cm^{-1}. Several lines of the detector were illuminated, however these were binned on board into two spectra, because of telemetry limitations. During an occultation, SOIR could measure up to four different orders (spectral intervals) every second, resulting into eight spectra downlinked to the Earth. Each of these measurements was obtained at the terminator at a local solar time of 6 AM or 6 PM; all latitudes were well covered, except for the 30° – 60° North region, due to the geometry of the spacecraft orbit. The vertical resolution, i.e. the vertical altitude range sounded by the projected slit at the limb on the atmosphere at the time of a measurement, varied from a few hundreds of meters for measurements at the North Pole up to 20 km when reaching the South Pole. The vertical sampling, i.e. the vertical distance between the mean altitude of two successive soundings, was also latitude-dependent, having values of approximately 2 km close to the North Pole, ~500 m between 40° and 70° North, and rising up to 5 km close to the South Pole.

The ASIMAT algorithm has been developed to study the SOIR spectra [41]. It is an iterative procedure, that fits the logarithm of the number density in each layer sounded during one occultation. Its uses simultaneously all spectra acquired during an occultation using the Bayesian algorithm Optimal Estimation Method (OEM), in a so-called onion peeling configuration [42-44]. The vertical resolution is taken into account by calculating the synthetic spectra on a discretization of the slit projection in the atmosphere [43]. For each species, the different density profiles deduced from the different possible orders are combined using a weighted linear moving average procedure on ± 2 scale heights [42, 44].The temperature profiles are derived from the CO_2 density profiles using the hydrostatic law.

SO_2 presents a weak band in the SOIR wavenumber sensitivity range, in the 2458 to 2525 cm^{-1} region. The SO_2 signature in the SOIR spectra is close to the instrument detection limit, i.e. close to the noise level. Moreover, the SO_2 features are completely overlapped by CO_2 absorption lines also present in this spectral range. A specific procedure has been developed, and is extensively described in [29]. In a first step, the spectra are fitted not considering SO_2, and the atmosphere conditions such as temperature and pressure profiles are determined using the iterative procedure described above. The spectra are fitted in a second step considering CO_2 and SO_2 together. A procedure using the spectral inversion degrees of freedom of the OEM algorithm is applied to discriminate between true detection and upper limit values at each altitude level. The SO_2 number densities at the altitude levels at which this criterion is not satisfied are considered as upper limit values. The SO_2 profiles are only provided for true detection values. The full sensitivity study is presented in [29]. In Figure 4, the filled markers are occultations for which a SO_2 true detection has been observed, while empty markers are measurements that only returned upper limit profiles.

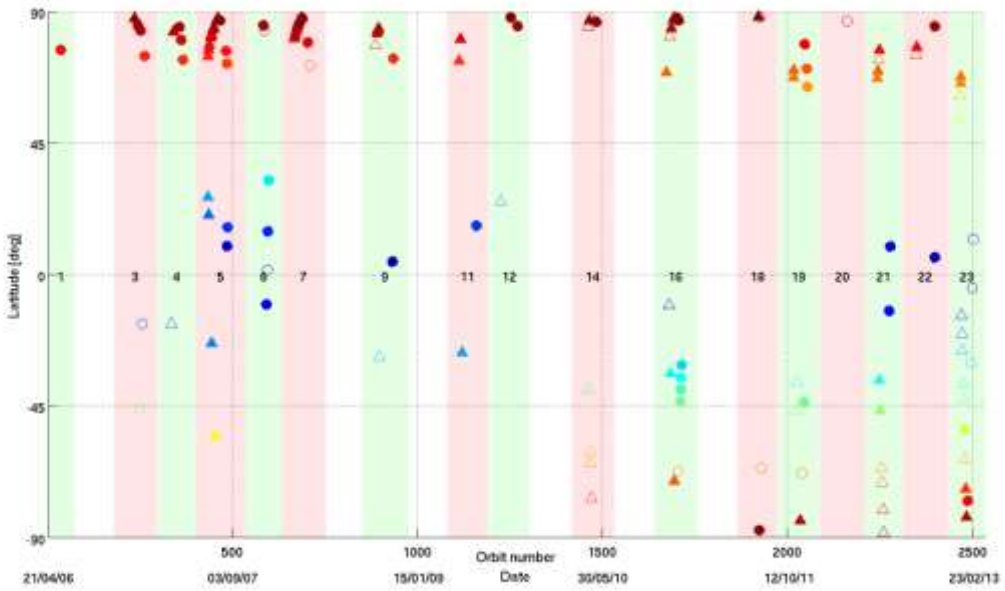

Figure 4: Localization of the SOIR SO_2 measurements, orbit number versus latitude. The date is also given as an indication. The occultation season numbers are also indicated in the middle of the plot. The colour code is the absolute latitude (dark blue at the Equator to dark red at the Poles), the circles denote measurements at the morning terminator, and the triangles are for the evening terminator. Filled markers are for positive detections of SO_2, unfilled for no detection (only upper limits).

3.2 SPICAV/UV

The SPICAV instrument on board VEx was a spectrometer very similar to SPICAM, part of the payload of the Mars Express orbiter [26, 45]. Its UV channel operated in the 118-320 nm

spectral range with a resolution of 1.5 nm at nadir or stellar/solar occultation modes. The CCD matrix of the spectrometer had 384 (spectral columns) x 288 (spatial lines) of useful elements with a spectral sampling ~0.5 nm per pixel. During one measurement, a fixed part of the detector recorded the signal which is grouped spatially in 5 bands by using binning of 2, 4, 8 or 16 lines of the matrix. Thus, at each second of an observation, 5 atmospheric spectra were obtained, spatially separated by latitude/longitude (in nadir mode) or by altitude (in occultation mode). The higher the binning factor (e.g. 16) the higher the signal to noise (SNR) ratio (maximum ~10^3), but the lower the spatial resolution.

Several absorption bands of SO_x (SO and SO_2) molecules are covered by the SPICAV UV spectral range: electronic transition bands $B^3\Sigma^- - X^3\Sigma^-$ (190-240 nm) and $A^3\Pi^- - X^3\Sigma^-$ (240-260 nm) of the monoxide, and analogue bands $\tilde{C}^1B_1 - \tilde{X}^1A_1$ (190-235 nm) and $\tilde{B}^1B_1 - \tilde{X}^1A_1$ (250-340 nm) of the dioxide. The strongest absorption bands are located in the 190-235 nm interval for both gases. This interval is used for the simultaneous retrieval of SO and SO_2. The SO_2 band near 280 nm is weaker, but is nevertheless included into the forward modelling used in the fitting procedure [27, 36]. The different observation modes of SPICAV/UV and their corresponding data coverage are described below.

3.2.1 Solar occultation

SPICAV and SOIR performed solar occultation simultaneously, pointing their respective fields of view (FOV) in the same direction (Sun). Data coverage with latitude and occultation seasons is therefore almost the same as for SOIR (Figure 4) and SO_2 vertical profiles can be retrieved jointly in the 65-100 km altitude range [27]. Each of the five SPICAV CCD bands point to different areas of the Sun and correspond to different tangent altitudes. The transmission spectra are processed separately, and then retrieved densities are sorted into one altitude profile that is highly sampled (<1 km). Depending on the CCD binning factor and distance to the planet's limb, the vertical FOV varies from 0.5 to 15 km. For this study, we selected orbits with the altitude FOV less than one scale height of the atmospheric density (i.e. <4 km).

The data analysis and retrieval procedure for the UV solar occultation are described in [27]. In the forward modelling, five atmospheric parameters are fitted: densities of CO_2, SO_2 and SO plus aerosol optical depth using the Angstrom coefficient formalism (expressing the spectral dependence of the aerosol extinction). Since at λ<180 nm, the signal from the solar radiance is too weak, we consider only longer wavelengths of the atmospheric transmission. This restriction prohibits us from detecting CO_2 abundance above 100-110 km where it strongly absorbs at λ<180 nm. On the other hand, below 85-90 km, the aerosol slant opacity becomes too high (>1) in the UV producing noisy signal at the level of the CCD's dark current. Thus, the most accurate results for SO and SO_2 mixing ratios are obtained between 90 and 100 km. One more uncertainty is linked to the overlap of SO and SO_2 absorption features in 190-230 nm. However, a correlation analysis for SO and SO_2 transmission spectra is applied [27]. The

retrieved dioxide abundance is therefore sensitive to the presence or absence of the monoxide abundance.

3.2.2 Stellar occultation

The stellar occultation technique is similar to the solar one with the difference that the star is observed as a weak point source. Only the night side of the atmosphere is probed. The instrument's FOV was directed to an UV star with high radiance at wavelengths within 100-300 nm (that is an advantage versus the spectrum of the Sun). Atmospheric density and temperature profiles were retrieved between 90 and 150 km [46]. The SO_2 analysis is performed from the same dataset as presented in that paper but at altitudes between 85 and 105 km. In order to accumulate more light from the star, the spectrometer's slit was removed. The spectral resolution is therefore larger than 2 nm. This does not allow distinguishing between SO and SO_2 features. In the forward modelling, the SO density is fixed at1% of the fitted SO_2 density. The same parameters are fitted as in solar occultations, plus the ozone abundance near 250 nm which is detectable by SPICAV/UV at the night side [47]. During the VEx mission, stellar occultation mode occurred regularly with different target stars, covering latitudes from 80°S to 80°N and local solar times from 19:00 PM to 05:00 AM (Figure 5).

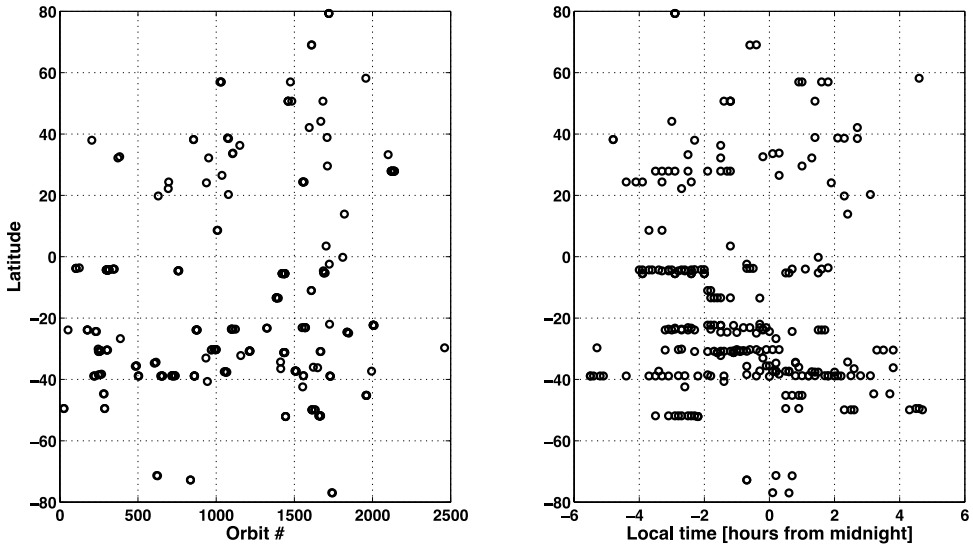

Figure 5: Localization of the SPICAV-UV SO_2 measurements in stellar occultation: latitude versus orbit number (Left Panel) and local time on Venus (Right Panel).

3.3 VIRTIS-H

VIRTIS [55] was a dual-channel spectrometer on board *Venus Express*. The low resolution channel VIRTIS-M was an imaging spectrometer working in the visible and near infrared at a moderate spectral resolution, whereas VIRTIS-H was an echelle grating spectrometer with a much smaller FOV, but a ten times higher resolving power (R~2000) from 2 to 5 µm. This

spectral range encompasses a SO_2 absorption feature around 2.45 μm. This absorption is located in the edge of a CO_2 transparency window that enables minor species measurements on the night side of the planet between 30 and 40 km, using the thermal emission from the hot lower atmospheric layers as a source. Unfortunately, SO_2 absorption in this region is spectrally narrow, so that only VIRTIS-H was able to measure SO_2 on its dispersion orders 5 and 6. This was done (among other minor species) by [30], using data from 44 orbits acquired during the earliest part of the nominal science mission (until early 2007). The orbital position was off-pericenter observations (totalling 50 % of processed VIRTIS-H observations) and pericenter observations (totalling about 27 %). These observations were also co-added in order to reach a sufficient SNR (about 100). Post-processing is minimal, and involves mainly the determination of the zero-intensity level so that the various dispersion orders agree with each other. These observations were then compared to a look-up table of pre-computed synthetic spectra in order to fit the abundance of various minor species (CO, OCS, H_2O, SO_2), as well as local vertical gradients for CO and OCS. The radiative transfer model used is the same as in [48, 49]. Both dispersion orders were used separately, and the co-located retrievals were then merged in order to increase their accuracy.

3.4 JCMT

Ground-based, sub-mm wavelength spectroscopic measurements of Venus SO_2 have been made with the James Clerk Maxwell Telescope (JCMT) since 2004. The JCMT, located on Mauna Kea, Hawaii [50], has a 15 meter primary mirror, providing diffraction-limited 14" spatial resolution at SO_2 line frequencies (346.65217 and 346.52388 GHz, observed simultaneously, see Figure 6). Data are collected at spectral resolutions ranging from 30 to 500 KHz (corresponding to bandwidths 250 - 1000 MHz). SO_2 abundances retrieved from 17 observation dates in the period 2004-2008 were presented in Sandor et al. [33]. These JCMT observations provided the first detections of upper mesospheric/lower thermosphere increases in Venus SO_2 and SO. Analysis of 2009-2014 observations is in progress.

Observed sub-mm spectra correspond to spectrally resolved absorption in the (colder) Venus mesosphere from the spectrally featureless, continuum emission originating from the deeper (warmer) atmosphere. Such spectra are pressure broadened (such that SO_2 altitude distribution is retrieved based on the shape of the observed absorption lines), and are therefore fundamentally sensitive to mixing ratio and not to number density. The SO_2 measurements are retrieved primarily from the stronger of the two SO_2 transitions (346.652 GHz), which does not overlap with any spectral feature from either the telluric or Venus atmospheres, see Figure 6 for several examples of spectra illustrating the high variability of both SO and SO_2. The weaker transition (346.524 GHz) has no telluric interference, but does compete with a Venus atmospheric SO feature (when SO is present), from which it is separated by only 4 MHz.

Temperatures used in the retrieval of SO and SO_2 are based upon JCMT temperature measurements, which themselves are retrieved from simultaneous, collocated observations of ^{12}CO (346 GHz) and ^{13}CO (330 GHz) [51]. Optically thin SO_2 absorptions have only weak sensitivity to temperature, the associated uncertainty being 7%.

Retrievals from Venus spectra show an altitude inversion, with SO_2 found only above 85 km, altitude invariant over 85-100 km, and with abundances varying from ≤2 ppb to 70±6 ppb [33]. No SO_2 is directly detected below 85 km. Interpretation of this non-detection is dependent on the assumed SO_2 altitude profile at the lower altitudes. The altitude region best determined from the observed SOx absorption lines is 85-100 km, but the detailed profile sensitivity depends on uncertain abundances above and below, and on the shape of the profile (e.g. [51]). If the altitude profile were linear below 85 km, then non-detection would indicate that the 70-85 km SO_2 is always ≤2 ppb. If SO_2 decreases exponentially with altitude in the 70-85 km range (as indicated by previous UV cloud top data (e.g. [4, 52]), then fitting of the JCMT data constrains the SO_2 abundances immediately below the ~ 80-85 km inversion altitude to be much smaller than the abundances directly above it, but puts no constraint on the SO_2 mixing ratios at 70 to ~80 km. In conclusion, it should be reminded that the fit to the sub-mm data cannot distinguish between a non-zero exponentially decreasing SO_2 density and a linear SO_2 density equal to zero in the altitude region below 80 km.

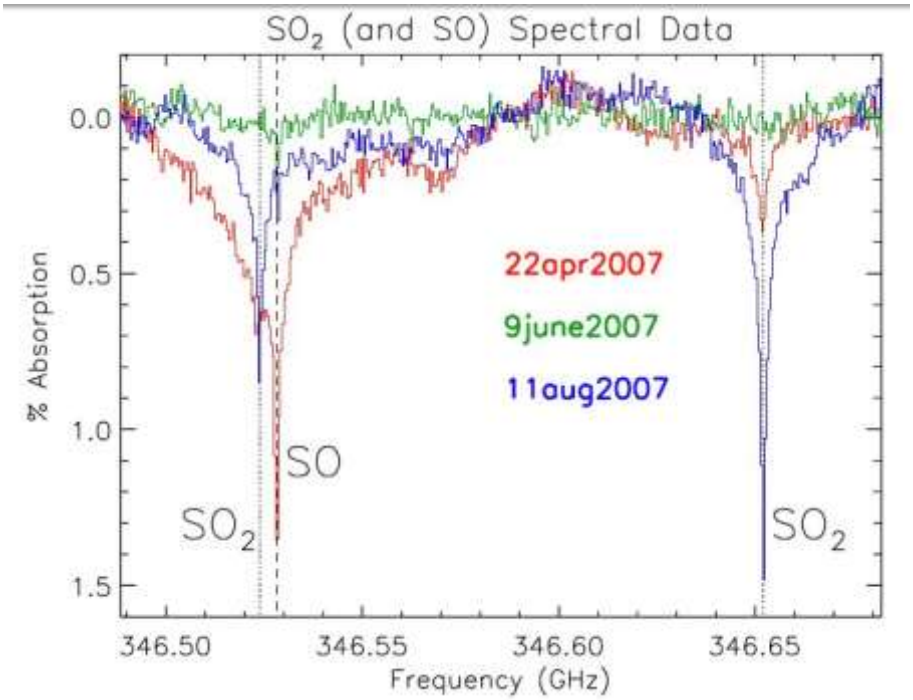

Figure 6: Venus spectra from 22 April (red), 9 June (green), and 11 August (blue), 2007, as measured by JCMT. Vertical lines indicate transition frequencies of SO_2 (dotted) and SO (dashed). Differences among the three spectra illustrate SO_2 temporal variation (30±5 ppb in April, ≤ 2 ppb in June, and 66±5 ppb in August). Comparison with the SO absorption demonstrates time variation among spectra can only be explained as time variation of abundance [33, 53]: Between April and August, SO_2 absorption increased, while SO absorption decreased. Any calibration error, or change in a background property of the atmosphere (e.g. temperature) would cause SO and SO_2 absorptions to change in the same

direction. Similarly, the June detection of SO (1.6±0.3 ppb) demonstrates that the simultaneous non-detection of SO_2 cannot be attributed to instrumental error.

Venus' diameter varies between 60" (full nightside) and 10" (full dayside), at inferior and superior conjunctions, respectively. Thus the JCMT's 14" resolution supports mapping of spatial variation across the mostly nightside disk when Venus is near inferior conjunction, but only disk-average measurements of the full dayside near superior conjunction. Observations made near half phase are obtained typically at two adjacent pointings, one to the dayside half-disk, and one to the nightside half-disk [54]. Disk average SO_2 abundances are time variable by a factor of 50 (≤2 ppb to 70±6 ppb) on a timescale of several months, and as much as a factor of 2 on a 1-week timescale (a 5-sigma result). On a 24 hour timescale, abundance variations are observed with confidence no higher than one-sigma. Time sampling at one-hour intervals show no variations. The only consistent pattern found to date is that the maximum SO_2 abundances at night are a factor of 2 larger than the maximum dayside values.

3.5 Other instruments

Other techniques and instruments have also been considered in this study. However they do not provide much information of the vertical distribution of SO_2 in the atmosphere, being more sensitive to the horizontal spatial distribution. Most of them provide information at given restricted altitudes. This is the case for example for the ground-based observations carried out with the ALMA [34] and TEXES [32] instruments and for the STIS instrument on the Hubble Space Telescope [31] or by nadir observations carried out by SPICAV/UV [26]. These instruments will be described in more details in Part II of this paper, where the analysis of their results will lead to the investigation of the spatial variability. However, some results obtained with these instruments will be used in the following discussion, allowing to reach a more global view of the SO_2 vertical distribution.

4 Comparison and discussion

The SO_2 VMR values obtained by the different instruments considered here are presented in Figure 7, where the instruments are represented by the different symbols and the colour code indicates the latitude at which the measurements were obtained. Day and night side observations have been separated for clarity. In these plots, the terminator evening side measurements have been considered together with the dayside measurements, while the terminator morning side measurements are with the night side measurements. Occultation measurements provide absolute densities, and hence VMRs if the total density is known. Observations with JCMT are sensitive to the vertical profile of the VMR and of the temperature, as described previously, and their interpretation relies on radiative transfer modelling. The uncertainties are not displayed in the figure, but Table 3 summarizes each instrument's typical uncertainty. As can be seen, values are quite high, reflecting the difficulty of such observations. The location of the measurements – latitude versus local solar time (LST) – is presented in Figure 9. Most of the measurements are localized on the dayside of

the planet and at the terminator, very few have probed the night side of the planet. Moreover gaps in observations near local noon and south of 60S are also clearly identified.

Instrument	**Typical uncertainty range (%)**
JCMT	9 – 100
VEx/SOIR	20 – 200
VEx/SPICAV-UV solar	10 – 100
VEx/SPICAV-UV stellar	10 – 100

Table 3: Uncertainty on the SO_2 VMR values of the different instruments is given in percent.

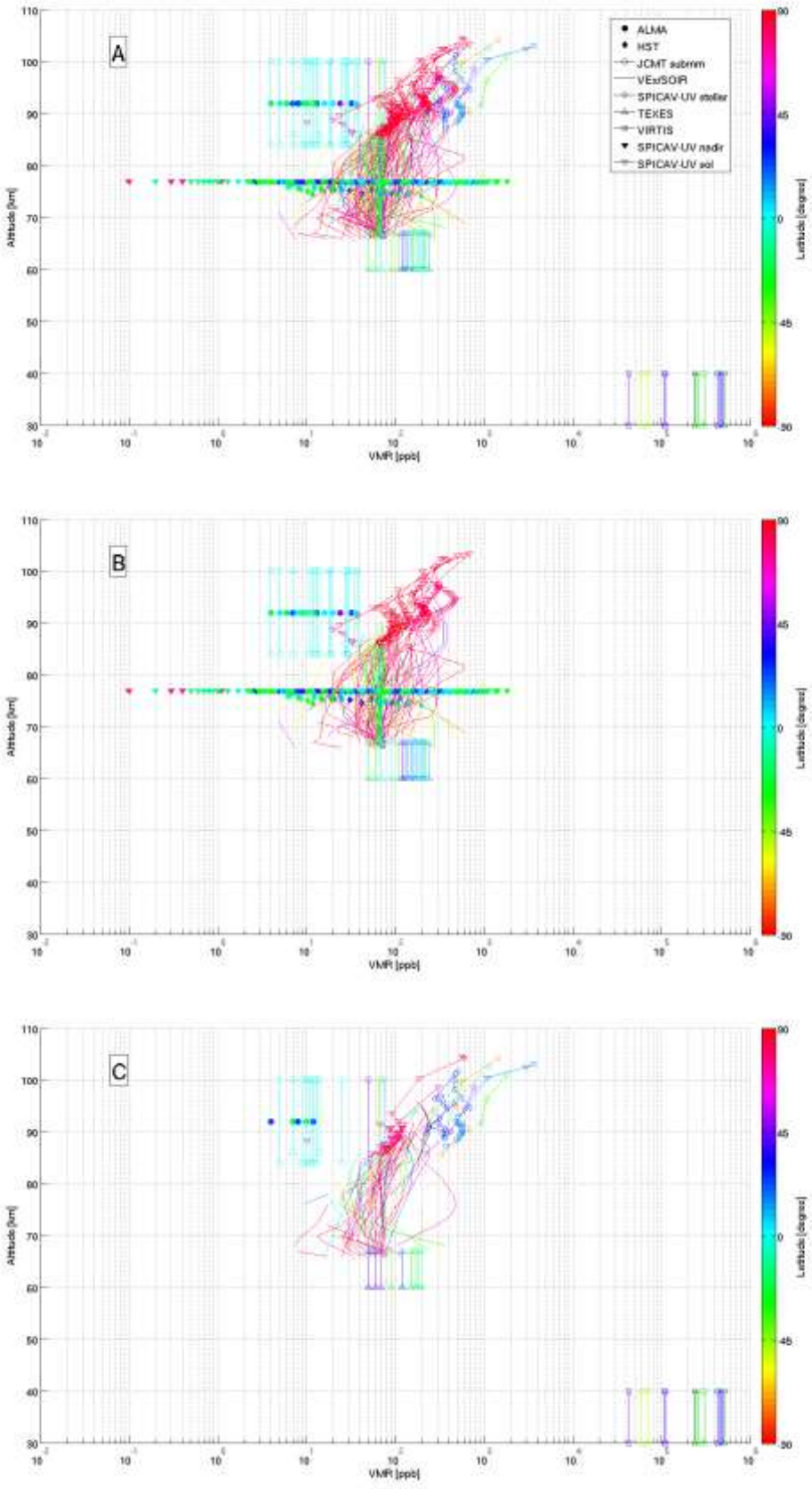
A
B
C
ALMA
HST
JCMT submm
VEx/SOIR
SPICAV-UV stellar
TEXES
VIRTIS
SPICAV-UV nadir
SPICAV-UV sol
Altitude [km]
VMR [ppb]
Latitude [degree]

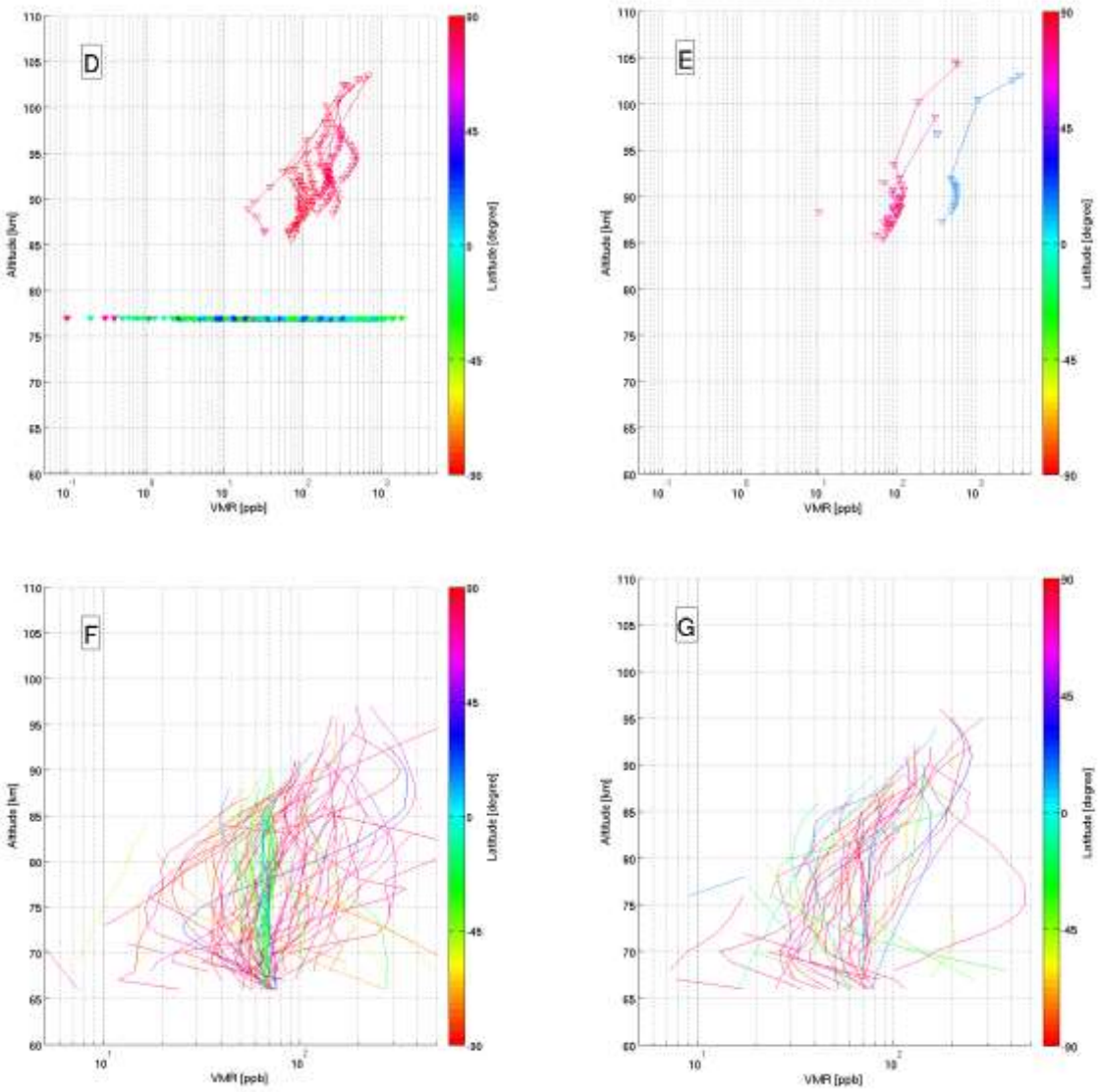

Figure 7: SO_2 volume mixing ratio as a function of altitude for the different instruments (symbols). The colour code is the latitude. Note that the JCMT measurements have a wide field of view, typically a few tens of degrees, centred on the Equator. Panel A: All data with no distinction of day/night. Panel B: day and evening side of the terminator measurements. Panel C: night and morning side of the terminator measurements. Panels D and E: Only SPICAV-UV, dayside and evening terminator (panel D) and night side and morning terminator (panel E). Panels F and G: Only SOIR, evening terminator (panel F) and morning terminator (panel G).

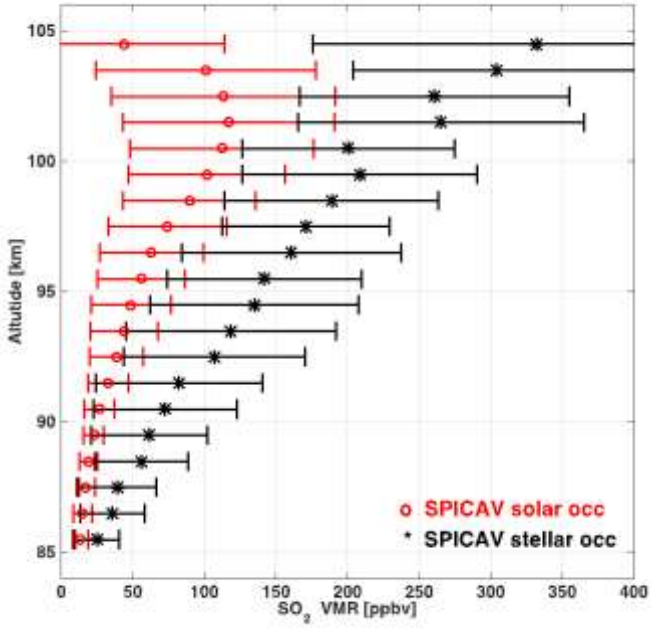

Figure 8: Vertical distribution of SO_2 volume mixing ratio (VMR) from SPICAV UV solar (in red) and stellar (in black) occultations. "Circles" and "stars" are the weighted mean values at each altitude considering the full data set. Horizontal lines are standard deviations. These results were retrieved after reprocessing of SPICAV occultation data that is described in detail in Belyaev et al. [55]

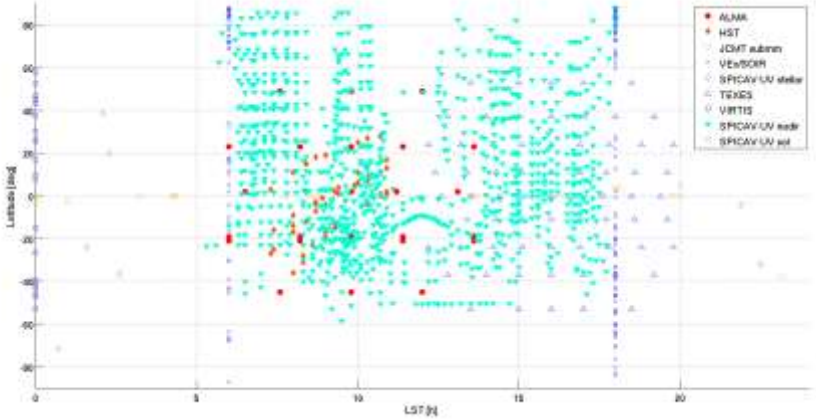

Figure 9: Geolocation of the SO_2 datasets, latitude as a function of local solar time (LST). The colour code as well as the symbols represent the different instruments. Note that (1) The VIRTIS observations were arbitrarily placed at midnight; (2) the JCMT measurements have a wide field of view, typically a few tens of degrees, centred on the Equator. For the altitude coverage of each instrument, the reader is referred to Figure 3.

In Panel A of Figure 7, the SO_2 VMR retrievals from all datasets are displayed independent of the observing geometry or wavelength of the actual observation platform. In this panel it is obvious that a wide range of SO_2 values is associated with each observation platform, spanning 2 to 4 orders of magnitude. As discussed previously, the data obtained from each platform was taken over a range of dates and locations. The breadth of observed values therefore emphasizes the strong temporal and spatial variability of SO_2 in Venus' atmosphere. Additionally, unlike the occultation observations which collect data as a function of altitude by scanning through different altitude levels, each of the nadir viewing observations samples a broad range of altitudes within a single observation, where the altitude sensitivity is defined as a function of the observational wavelength. For example, ground-based observations in the infrared (TEXES) probe the lower mesosphere above the cloud top at altitudes of 60-85 km at 7 μm or a few km below starting from within the clouds to about 85 km at 19 μm. These IR data essentially deliver a column abundance above the continuum formation level (roughly the cloud tops) and provide limited information on the vertical gradient of the SO_2 gas. Likewise, the HST/STIS data essentially deliver the column abundance above the unit optical depth altitude of the cloud tops. In contrast, sub-mm observations probe the upper mesosphere above an altitude of 80 km, however constraints on the shape of the gas density profile both above and below 80 km can also be inferred from the analysis of the spectral model fits to the data. However it should be noted that reduction of the sub-mm data is also sensitive to the assumed temperature profile.

Thus, while the occultation data provide the most direct sampling of the gas profile as a function of altitude above ~ 65 km, the nadir observations provide contextual information at altitudes and local times not probed by the occultation observations. For example, comparison of the 7 μm TEXES data and the (2-5 μm) VIRTIS data taken over a range of local times indicates that the strong decrease within the cloud layer, from ~10^5 ppb at 40 km to ~100 ppb near 60 km, appears to be stationary in the atmosphere (Figure 7C). The vertical profile inferred from the occultation data generally has a minimum around 70-75 km with values ranging between <10 and 500 ppb, above which an increase is observed in most of the profiles to reach 600 - 4000 ppb at 105 km (Figure 7C-E). This type of inversion is directly implied by the analysis of the sub-mm data obtained by JCMT and ALMA [31, 33, 34] and is also supported from nadir viewing observations taken in the UV by SPICAV and other Earth based platforms with the ground based sub-mm and IR observations. But, due to the strong temporal and spatial variability of the atmospheric SO_2 abundance in the 70-75 km altitude range, comparison of the SO_2 retrievals inferred from multi-wavelength nadir platforms probing the 70-100 km altitude range is only valid when comparing datasets taken at the same temporal epoch over the same spatial regions as was done during the HST-JCMT-Venus Express SO_2 observing campaign in 2010/2011 [31].

From Figure 7C-E, we see that there is significant overlap in the range of SO_2 VMRs observed throughout the VEx mission from the morning and evening sides of the terminator, and night side observations. There is good agreement between the night side and terminator

SPICAV-UV stellar, SPICAV-UV solar, SOIR and dayside and night side TEXES VMR values in the 60 – 105 km region, even if in general, SPICAV-UV stellar observations lead to higher values above 85 km. We also point out that the values from SPICAV-UV solar and stellar, are being reprocessed to better take into account the contributions of stray light within the SPICAV instrument and also of light coming from different altitudes of the atmosphere and being scattered within the field of view of the instrument [55]. First results [56] indicate that the SO_2 inversion is confirmed (see Figure 8), with abundances between 10 and 30 ppb at 85 km increasing to 100-300 ppb at 100 km, getting in better agreement with the JCMT and ALMA data in the 85-90 km range. Although the haze extinction is approximated by a power function in Belyaev et al. [27], which is a reasonable approximation, other options [57] based on Mie calculations could affect the retrieval. Also, although it is not clear from the SOIR individual VMR profiles in Figure 7, the inversion is also supported by the SOIR latitude binned mean profiles, that are not plotted in this paper but can be found in Figure 9 of [29].

The SO_2 mixing ratios retrieved from the sub-mm (JCMT and ALMA) observations, however, are consistently about a factor of 10 – 50 (or with the new analysis 2-25) times smaller than those retrieved from the occultation observations made at the terminators or on the nightside. While it is important to keep note that the sub-mm analysis is sensitive to the assumed temperature profile, it remains that specific constraints on the vertical gradient can be inferred from the sub-mm data. As discussed previously, JCMT results (which average over multiple local times) are not compatible with a strong increase of the SO_2 abundance with altitude such as is reported by SOIR and SPICAV-UV occultations (which obtained data over a very limited local time period). These differences are provocative and suggest that it is important to understand how/if local time impacts the shape of the vertical SO_2 profile.

And while additional improvements in the SPICAV-UV occultation retrievals may be forthcoming, the new results will not resolve the differences between the slope in the vertical profile inferred from SPICAV-UV and that needed to fit the JCMT sub-mm data. In particular, additional diffused light from the forward scattering by the haze which is present below 100 km may be contributing in a small way to the signal recorded in the SPICAV-UV occultation spectra. This effect, which has not yet been taken into account, it may impact the currently retrieved CO_2 densities (CO_2 densities will be higher after correction). This would introduce a systematic difference in the VMR profiles below 100 km altitude. The retrieved SO_2 VMR values would decrease below 100 km after correcting the CO_2 retrieval bias, but the retrieved SO_2 VMRs above 100 km would not be impacted much. Thus, the slope of the retrieved SO_2 VMR increase near 100 km would steepen further suggesting a pronounced inversion in the SO_2 abundance above 80 km in contradiction with the JCMT findings.

In spite of the contradiction between the SO_2 profile gradient needed to fit the sub-mm data and that retrieved empirically from the SPICAV-UV and SOIR occultations, the latter two datasets do agree on the existence of an inversion at high altitude. This correspondence comes even though the SPICAV data considered here are both stellar and solar observations and do not all correspond to the same latitudes and local solar time as the ones probed by the SOIR

instrument. Moreover, both instruments probe the atmosphere in different spectral ranges (UV-IR) and derive the SO_2 VMR using totally different retrieval algorithms. Both are based on the occultation technique which provides 'auto-calibrated' transmittances, from which most of the instrumental effects have been removed by dividing the atmospheric spectrum by an out-of-atmosphere reference obtained during the same occultation sequence. The profiles are acquired with an altitude resolution that depends on the observation geometry (distance from Venus) without requiring any assumptions on the slope or scale heights of the retrieved densities. Moreover, SOIR uses temperature profiles directly derived from its own measurements. Indeed, as explained in the previous section, temperatures are deduced from the SOIR observations through the hydrostatic law applied on the retrieved CO_2 densities. No specific assumption is needed, contrary to the analysis of the sub-mm data which requires some hypothesis on the vertical temperature and VMR profiles. Moreover, CO lines are used to constrain the temperature in the analyses of the sub-mm data.

Given these facts, we also suggest that the sensitivity of the JCMT temperature profiles to the constraint (initial temperature profile) needs to be investigated. The required follow-on investigations must also define the impact of the uncertainty in the temperature retrievals (which rely on disentangling the CO and temperature profiles) on the fit SO_2 VMR. This work, while needed, is beyond the scope of this paper.

We emphasize that in this study only the SO_2 VMR values associated with positive SO_2 detections are shown. This is true for all instruments, and in particular for SOIR and SPICAV-UV, which have the largest data sets. The upper limit values, which could be derived for non-detection observations, are not displayed for the sake of clarity. Calculating mean profiles should consider these upper limits in order not to introduce a bias. This should be done for all data sets, but has not been considered in this study, being outside the scope of this work.

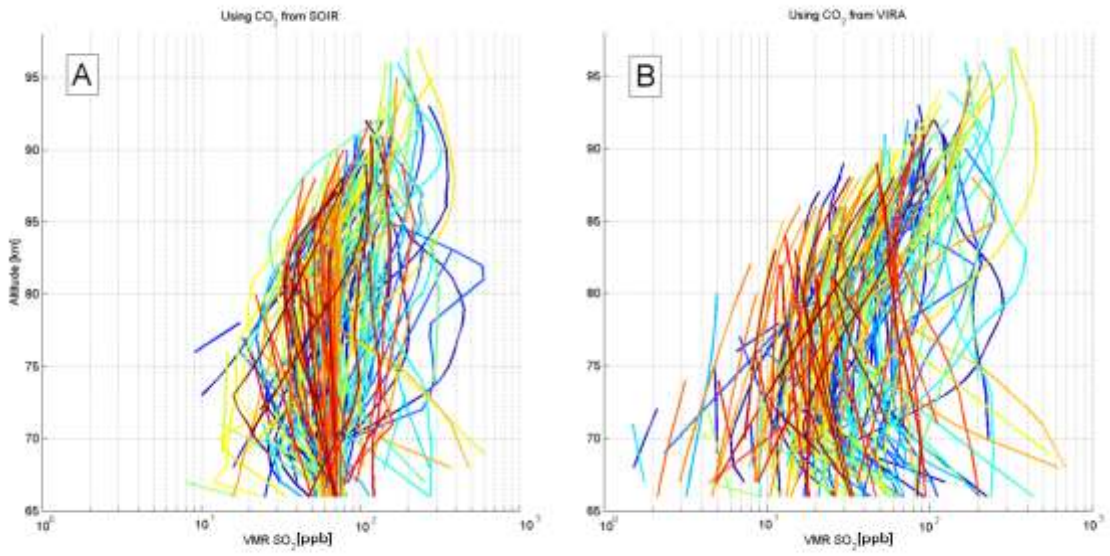

Figure 10: Comparison between the SOIR SO_2 VMRs when calculated using the SOIR simultaneously measured CO_2 densities (Panel A) or using the CO_2 densities from the VIRA model (Panel B). Colour indicates latitude (see colour scale in Figure 7).

It is also important to note that the VMR values of SOIR and SPICAV-UV stellar and solar observations are obtained by measuring simultaneously the CO_2 and the SO_2 number densities, and assuming the CO_2 VMR (equal to a constant 96.5% for the altitude range considered here, as given in the VIRA model) [27, 43, 44]. For the SOIR instrument, the temperature profile is derived directly from the CO_2 densities using the hydrostatic equilibrium equation [43]. The CO_2 number density profiles are only derived from non-saturated spectral lines, and are thus limited to the ~70 km to 120 km region. The CO_2 number density profiles are then extended hydrostatically to lower altitudes, assuming an extrapolated temperature profile which has the same gradient as the VIRA temperature profile. In general, the SO_2 VMR is calculated with reference to the CO_2 abundance measured during the same occultation, in order to account for the variation in CO_2 density. However, as has been shown in [43, 44], the SOIR CO_2 number density profile retrievals differ from those found in the VIRA atmosphere [58, 59]. Therefore, in Figure 10, we compare the SO_2 VMR profiles derived using the SOIR CO_2 (Panel A) and the (constant) VIRA CO_2 (Panel B) densities. Using the CO_2 profiles from SOIR or from VIRA does not change much the slope of the individual profiles. This is expected since the scale height is approximately the same for both VIRA and SOIR CO_2 profiles. The variability when using CO_2 from VIRA (mean geometric standard deviation is 2.3) however is much larger than when using CO_2 from SOIR (mean geometric standard deviation is 1.8). This advocates for the use of CO_2 measured along with the other trace gases and for an in-depth revision of the VIRA model.

5 Theoretical modelling and interpretation of observations

Photochemical modelling is the primary tool for defining the chemical processes that support the spatial distribution and abundance of the sulfur-oxide species, molecular oxygen (O_2) and H_2SO_4 observed in Venus' atmosphere. The recent observations described in the previous sections have sparked a resurgence of interest in modelling sulfur chemistry on Venus. In the following we will use several 1-d photochemical models with simplified (specialised) or comprehensive photochemistry [60-62], a 3-d GCM with full photochemistry and simplified microphysics,[63, 64] as well as parametric studies using tracers with specified lifetimes in simplified dynamical models [37], see Table 4 for a summary of their characteristics. Two models [60, 61] continued the effort to understand the global-scale chemical processes operating in Venus' mesosphere and the links among the polysulfur, sulfur oxidation, and carbon cycles [65]. Three [60, 62, 66] assessed potential mechanisms for creating the observed vertical profiles of mesospheric SO_2 and SO; one [67] evaluated the potential implications of interactions between water and SO_2 for the chemical state of the mesosphere; and one [31] simulated the expected variation of SO_2 and SO with local solar time.

Table 4: Summary of the Models used or cited in this study. * indicates that the model includes temperature-dependent cross-sections for photoabsorption and photodissociation

Model	Type	diurnal cycle	Description	Altitude range	T	Type of chemistry	Dynamics	Cloud microphysics	Ref
Caltech/JPL Photochemical Model (KINETICS)	1-d	Global average	46 species - 405 reactions*	58-112	specified	Comprehensive photochemistry	N	N	Mills and Allen, 2007 [61]
	1-d	Diurnal average at 45° latitude	24 species - 218 reactions	58-112	specified	Simplified sulfur photochemistry	N	N	Zhang et al, 2010 [66]
	1-d	Diurnal average at 70° latitude	49 species - 414 reactions -	58-112	specified	Comprehensive photochemistry	N	N	Zhang et al, 2012 [62]
	1-d	Diurnal average at 70° latitude	36 species - 280 reactions	58-112	specified	Comprehensive sulfur and water photochemistry	N	N	Parkinson et al , 2015 [67]
	1-d	SZA dependent	24 species - 218 reactions	58-112	specified	Simplified sulfur photochemistry	N	N	Jessup et al, 2015 [31]
LMDLMD Venus GCM	3-d	Y	33 species - 140 reactions*	0-100 (140)	calculated	Comprehensive photochemistry	Explicit	Y (simplified)	Stolzenbach et al., 2014 [64]
Krasnopolsky Mesosphere Model	1-d	Global average	44 species – 153 reactions	47-112	specified	Comprehensive photochemistry	N	N	Krasnopolsky, 2012 [60]
Krasnopolsky Lower Atmosphere Model	1-d	Global average	28 species – 89 reactions	0 – 47	specified	Lower atmosphere chemistry	N	N	Krasnopolsky, 2013 [68]

A comparison between the measured and modelled vertical profiles is presented in Figure 11 to better visualize the overlap between models and observations. Both are comparable in magnitude at 75-100 km; at 60-75 km, the modelled range from the Parkinson et al. model (for high latitudes) is significantly larger than has been observed at either low to mid-latitudes (0-45°) or at mid to high-latitudes (45-90°). It should be noted that the SO_2 VMR ranges inferred from the models and observations arise from two very different sources. For models, the plotted range arises from different assumptions regarding the chemistry, eddy transport, and boundary conditions. For observations, the range arises from temporal, geographic, and local solar time variations, as well as systematic differences amongst measurement techniques.

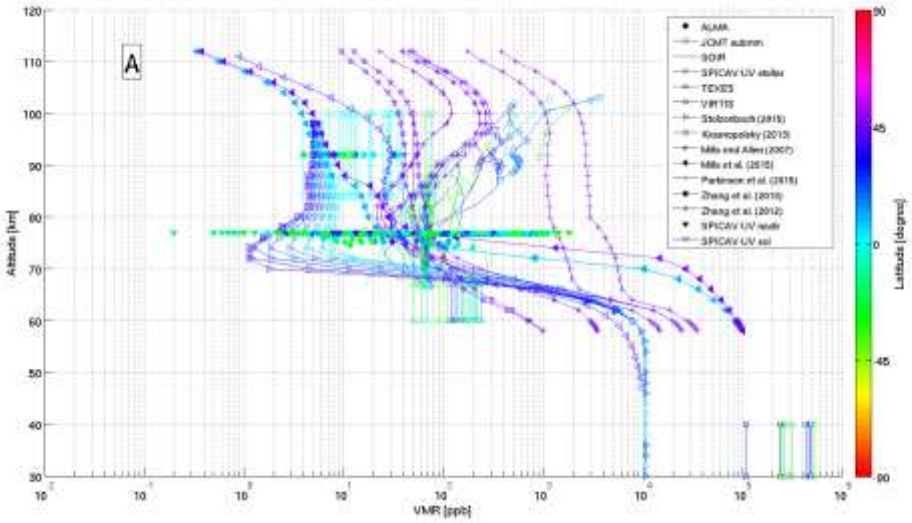

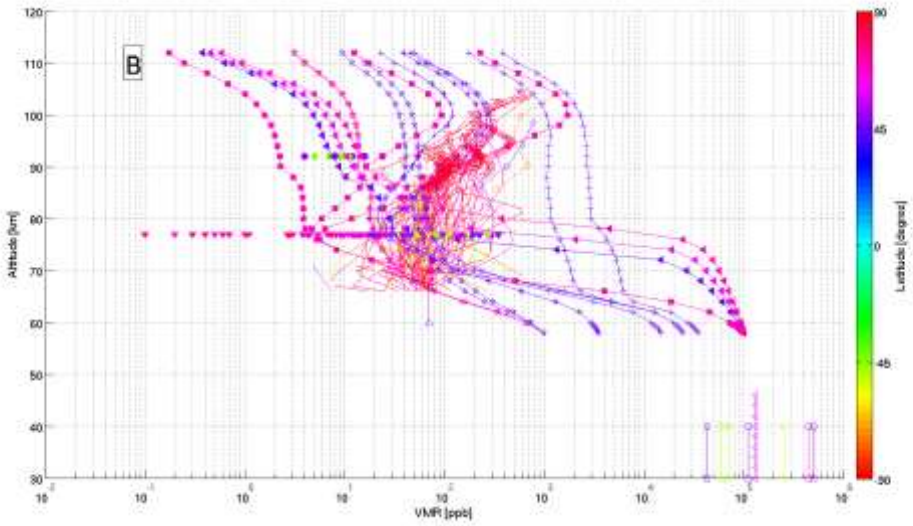

Figure 11: All VMR profiles from datasets and models as a function of the altitude. The colour code is the latitude. Panel A: Low latitudes (lower than 45°). Panel B: Higher latitudes (higher than 45°). Stolzenbach 2014 [64] = range of latitudes but could split them at 38 deg; Krasnopolsky 2012 [60] – 38 deg; Krasnopolsky 2013 [68] – both plots ; Mills and Allen 2007 [61] – 45 deg ; Parkinson 2015 [67] – 70 deg ; Zhang 2010 [66] – 45 deg ; Zhang 2012 [62] – 70 deg

Only two models [64, 69] simulate the SO_2 VMR value below 45 km. In each case the model predicted VMR is constant over the simulated 30-45 km altitude region; however, the magnitude of the VMR is different for each model (Figure 11). This is an indication of differences in the assumed lower boundary conditions between the two models. For the remaining models, whose lower boundary is at 58 km, the two orders of magnitude differences amongst the models also largely reflect that different assumptions were made for the SO_2 VMR at each model's lower boundary altitude. For example, in some cases the lower boundary condition for SO_2 was chosen so that the modelled SO_2 VMR at the cloud top (~ 70-75 km) would be within the 10-100 ppb range that has been typically observed.

The TEXES and VIRTIS observations, in combination, place very stringent constraints on the behaviour of SO_2 through the lower and middle clouds. These observations imply that SO_2 VMRs decrease by three orders of magnitude between 30 and40 km and above 67 km. Although the SO_2 VMRs predicted by the Krasnopolsky model [69] are by assumption consistent with the VIRTIS retrievals between 30 and 40 km, no model comes close to simulating the dramatic decrease in the SO_2 VMR observed between 40 and 67 km. The cause of the loss of SO_2 over 40–67 km is currently ill-defined. It cannot simply be oxidation to H_2SO_4 because the H_2O abundance in the troposphere is about one-quarter to one-fifth of the tropospheric SO_2 abundance and the SO_2 photolysis rate decreases rapidly below its peak near 65 km in models [61, 62]. Thus, there must be some other aspect of the modelling that should be adjusted to create agreement between the models and the observations.

Most theoretical models do recreate a rapid fall in SO_2 VMR with height, but they concentrate the gradient near 65-70 km rather than distributing the gradient over <57 to 70 km. The accuracy of this altitude assignment relative the available observations is dependent on the sensitivity of the spectral models used in the analysis of the data (such as the 7 μm TEXES data) to the gradient of the gas abundance profile. Interestingly, the sensitivity of the TEXES SO_2 gas abundance retrievals to vertical profile shape has yet to be thoroughly examined. Additionally the assignment of the minimum altitude probed by the TEXES IR data (e.g., down to 57 km at 19 μm) is based on the brightness temperature of the continuum (241 K, from [70]) and thus depends on the assumed temperature profile. However other temperature determinations, e.g. using VERA [71] or VIRTIS-M [72], indicate that the 241-K level at low latitudes is located at altitudes higher than 57 km (roughly 67 km according to Vera and 64 km for VIRTIS-M). Thus, a study of the sensitivity of the gas density retrievals and the modelled gas density profiles to the assumed temperature profile and the resulting cloud top altitude is also required. Each of these sensitivity tests would allow for clearer understanding of the relationship between the retrieved gas distribution, abundance and vertical gradient which in the end may lead to better agreement between the observations and the theoretical models.

At 75-85 km, model results for SO_2 fall into three clusters - larger than 100 ppb, 10-100 ppb, and less than 10 ppb - depending on the chemistry assumed:

(1) Modelled SO_2 at 75-85 km exceeds 100 ppb in calculations where there is a sufficiently large excess of SO_2 over H_2O at 60 km [67]. In these models, there is insufficient H_2O to convert a significant fraction of the SO_2 that is transported upward from the lower boundary into H_2SO_4. Consequently, the upward transport rate for SO_2 is much larger than in the other models.
(2) SO_2 at 75-85 km is less than 10 ppb in models with simplified sulfur chemistry [64, 66], suggesting the simplifications adopted in those models lead to an oxidation rate for SO_2, producing H_2SO_4, that is significantly faster than in the "comprehensive sulfur chemistry" models.
(3) The "comprehensive sulfur chemistry" models [60-62, 67] include metastable sulfur oxides (e.g., $(SO)_2$, S_2O, $ClSO_2$, and SO_2Cl_2) that lengthen the effective lifetime of SO_2 against oxidation to SO_3 above about 70 km. This increases the vertical transport rate for SO_2 in the "comprehensive sulfur chemistry" models compared to the highly simplified sulfur chemistry models. Another consequence is that these models have small vertical gradients for SO_2 over 75 to 90 km with the SO_2 VMR changing by less than a factor of two.

A prominent observational feature is the SO_2 inversion layer in which VMRs at 85-100 km are larger than those at 75-85 km. The magnitude and steepness of the inversion inferred from sub-millimetre and solar/stellar occultations differ, but, as discussed previously, all observational studies agree on the fact that the inversion layer exists (e.g., [31, 33], Section 4 of this manuscript). Analysis of the available TEXES data shows that there is a cut-off in the

SO_2 abundance at ~ 67 km, such that the SO_2 abundance above cannot exceed a few (2-4) ppb, which is much lower than the abundance observed above the cut-off altitude by other instruments. Thus, the combination of the TEXES and the sub-millimetre data analysis strongly suggests that there is a minimum inflection point in the SO_2 gas abundance between 70 and 80 km.

Three 1-d modelling studies produced SO_2 profiles with a significant inversion layer above 75 km: models A and B in Zhang et al. [62], models B and C in Zhang et al. [66], and the cases from Parkinson et al. [67] in which the water abundance equalled or exceeded the SO_2 abundance at 60 km. All three studies produced SO_2 profiles with a minimum near 75 km, a shape similar to that inferred from the solar occultation observations, and a maximum VMR at 95-100 km that is comparable to the maximum inferred from the solar occultation observations. In all three, the SO_2 inversion layer was induced by transporting sulfur in condensed phase as aerosol particles from below 75 km to above 75 km.

In Zhang et al. [66], the SO_2 inversion layer was induced by (i) increasing the H_2SO_4 visible wavelength cross section by a factor of 100; (ii) using the highest temperatures reported by SPICAV above 85 km to maximise the H_2SO_4 saturation vapour pressure, (iii) scaling the H_2SO_4 saturation vapour pressure to prescribe the vertical profile of gaseous H_2SO_4; (iv) selecting the H_2SO_4 saturation vapour pressure-temperature relation [73-76], that gave the largest H_2SO_4 saturation vapour pressure when extrapolated to Venus mesosphere conditions; and (v) assuming gaseous H_2SO_4 would be supersaturated by a factor of up to 10. With these extreme settings the models B and C of Zhang et al. [62, 66] produced SO_2 inversion layers similar to those inferred from the solar occultation observations, but require a gaseous H_2SO_4 abundance at 85-100 km that exceeds by several orders of magnitude the 3 ppb observational upper limit [53].

In Zhang et al. [62], the inversion layer was induced in two ways. One method was by (i) setting the H_2SO_4 cross section at 195-330 nm to its experimental upper limit [77, 78], (ii) using the highest temperatures reported by SPICAV above 85 km to maximise the H_2SO_4 saturation vapour pressure; (iii) scaling the H_2SO_4 saturation vapour pressure to prescribe the vertical profile of gaseous H_2SO_4; (iv) selecting the H_2SO_4 saturation vapour pressure-temperature relation [73-76] that gave the largest H_2SO_4 saturation vapour pressure when extrapolated to Venus mesosphere conditions; and (v) using a saturation ratio of 0.25. Similarly to the previous study by Zhang et al. [66], the SO_2 inversion layer obtained here by the model A of Zhang et al. [62] is obtained at the expense of a gaseous H_2SO_4 in large excess relative to the 3 ppb observational upper limit [53]. A similar result was obtained by Parkinson et al. [63] when the SO_2 abundance is not in large excess over the water abundance at 60 km.

The other method (model B) proposed by Zhang et al. [62] was by scaling the S_8 saturated vapour pressure by a factor of $3x10^{-4}$ to produce the observed SO_2 profile. This approach has the advantage of not requiring H_2SO_4 amounts greater than the observed upper limit.

However, it remains a highly speculative possibility since S_x aerosols have never been observed in Venus' mesosphere and the kinetics of the S_x chemistry is largely unknown due to the lack of laboratory data.

None of the other 1-d photochemical models, all of which are gas-phase only, has a significant SO_2 inversion. Furthermore, no model replicates the more extreme SO_2 inversion inferred from the SPICAV-UV stellar occultation, particularly the data obtained above mid-latitudes (Figure 7b, Figure 7a-e).

While all the models presented in Figure 11 show an exponentially decreasing SO_2 VMR between 60 and 70 km, only the [60, 61, 64] SO_2 profiles show a near constant SO_2 VMR between ~ 80 and 95 km (i.e., one that does not increase or decrease by more than a factor of 2 between these altitudes) that is within the observed SO_2 VMR range.

The LMD 3-d model at mid- to high latitudes [64] is the only one that has a significant inversion layer above 80 km which has not been prescribed. In this model the slope of the 75 to 85 km VMR profile increases with increasing latitude such that at middle and high latitudes a strongly increasing VMR profile is evident, but at the equator the profile is nearly constant between 75 and 85 km (Figure 11). The latitudinal gradient in the magnitude of the 75 to 85 km VMR profile slope seems to be a dynamical effect due to SO_2 or a precursor propagating to the upper mesosphere at equatorial latitudes and then being transported by the mesospheric equivalent of the Hadley circulation poleward and then downward to the lower mesosphere. Thus, the LMD model indicates that dynamics can produce a minimum inflection in the SO_2 VMR profile between 70 and 80 km and may play an important role in the observed inversion. The LMD model's near-constant SO_2 VMR profile at 70-95 km at the equator mimics the results derived from the Mills and Allen [61] and Krasnopolsky [60] photochemical models at 45 and 60 degrees solar zenith angle, respectively. Thus, it is evident that without significant manipulation of the physical properties of the atmosphere, no model has been able to produce a strong minimum inflection point at ~ 75 km based solely on photochemistry.

Dayside (non-terminator) observations of SO_2 above 85 km are entirely the purview of the sub-mm observations. Sub-mm observations reported by Sandor et al. [33, 79] show that variability in the SO_2 and SO gas abundances is inconsistent with SO_2 and SO comprising a closed system in which, for example, a decrease in SO_2 gas density results in an increase in the SO gas density. The correlated variability in SO_2 and SO gas abundances and variations in total SO_x ($=SO_2$ + SO) that are larger than an order of magnitude demonstrate that there must be another sulfur-bearing species above 80 km whose abundance is comparable to or larger than that of SO_2 and SO. Similarly, the HST/STIS observations obtained during the *Venus Express* era show for the first time that the cloud top (70-80 km) SO column density distribution is directly correlated with the cloud top (70-80 km) SO_2 density - rather than anti-correlated as would be expected if the SO_x balance was purely photo-chemically driven and SO_2 and SO were the primary/solitary sources of sulfur at these altitudes [31]. Thus, the HST

results extend the altitude range through which it should not be assumed that SO_2 and SO are the sole contributors to Venus' sulfur budget.

6 Conclusions

All observations presented in this compilation show a high degree of variability of the SO_2 profiles, both temporal and spatial. The most noticeable characteristics of the SO_2 profile detected from the available SO_2 observations is the existence of the SO_2 inversion layer in which VMRs at 85-100 km are larger than those at 75-85 km. The magnitude and steepness of the inversion inferred by different techniques differ, but all studies agree on its existence.

SO_2 abundance and spatial distribution in the Venus' middle and upper atmosphere are balanced between SO_2 loss via photolysis and oxidation to SO_3 – leading to the formation of the H_2SO_4 gas and aerosol - , local source mechanisms (e.g. kinetic SO+O reaction), vertical transport (e.g., eddy diffusion, convection), horizontal transport (i.e., zonal wind) and meridional transport. The observations presented in this compilation plainly indicate that at least one other significant sulfur reservoir (in addition to SO_2 and SO) must be present throughout the 70-100 km altitude region to explain the inversion in the SO_2 vertical profile at ~80 km, leading to unexpected increase in the SO_2 abundance above ~80 km [33, 34]. These results represent a new empirical constraint that must be replicated by models of Venus' sulfur oxide cycle.

The comparison of the photochemically modelled and observed SO_2 vertical profiles raises the following issues that require further study:

1. No viable photochemically modelled middle atmospheric (~ 70-100 km) source of SO_2 or SO has been identified or validated, but all the observations require that an additional middle atmosphere sulphur reservoir exists;
2. The observed temporal and spatial variations of SO_2, SO, [SO_2+SO], and SO/SO_2 are large. Recent modelling suggests that dynamics may play a role in the observed behaviour. However, a definitive and plausible explanation of the physical and/or chemical mechanisms driving the sulfur-oxides variations that is consistent with our current knowledge of the atmospheric characteristics does not yet exist;
3. Altogether, the observations suggest that there is a minimum inflection point in the SO_2 abundance between 70 and 80 km. No photochemical model has an explanation for this behaviour. GCM modelling indicates that dynamics may play an important role in generating an inflection point at 75 km altitude but does not provide a definitive explanation of the source of the inflection at all local times or latitudes;
4. Differences between the thermal structure and cloud models used for interpretation of observations and those used in photochemical models are significant and have important implications for understanding and modelling SO_2 on Venus;

5. The large range of SO_2 values resulting from photochemical models reflects significant uncertainty in our knowledge of sulfur chemistry on Venus.

In summary, we currently do not know what the other significant sulfur compound(s) may be nor do we know what other compounds may play important roles in the progression of the sulfur chemistry cycle, e.g., new reaction mechanisms that may serve as catalysts to the progression of the cycle have not yet been identified or validated. Halogen compounds [61, 80] and H_2O [67] have both been suggested as possible major players in the SO_x and S_x cycles but significant gaps in laboratory and observational data have hampered definitive quantification of their roles. Deeper understanding of these cycles will require the identification and mapping of related gaseous species (including H_2O, halogen species, and more) and particulates (hazes and clouds).

In Part II of this series, we will investigate in more detail the horizontal and temporal variability of the sulfur species within the Venus atmosphere.

Acknowledgements

The authors wish to thank the International Space Science Institute (ISSI) for their fruitful support. Most of the authors were members of the ISSI International Team "Sulfur Dioxide variability in the Venus atmosphere" which met during 2013-2015 in the facilities of ISSI in Bern, Switzerland.

Venus Express is a mission of the European Space Agency. The James Clerk Maxwell Telescope is operated by the Joint Astronomy Centre on behalf of the Science and Technology Facilities Council of the United Kingdom, the National Research Council of Canada, and (until 31 March 2013) the Netherlands Organisation for Scientific Research. Investigator Sandor was supported by the U.S. National Science Foundation under Grant no. AST-1312985, and by NASA under Grant nos NNX10AB33G, NNX12AI32G and NNX14AK05G. F.P. Mills also acknowledges partial support under NASA Grant NNX12AI32G to Space Science Institute. The research program was supported in Belgium by the Belgian Federal Science Policy Office and the European Space Agency (ESA, PRODEX program, contracts C 90268, 90113, and 17645). Some authors also recognize the support from the FP7 EuroVenus project (G.A. 606798). We acknowledge the support of the "Interuniversity Attraction Poles" program financed by the Belgian government (Planet TOPERS). This research was also supported by a BRAIN research grant BR/143/A2/SCOOP of the Belgian Federal Science Policy Office. A. Mahieux thanks the FNRS for the position of "chargé de recherche". O. Korablev, D. Belyaev acknowledge support from Roscosmos and the Russian Academy of Science (FANO). E.Marcq, F. Montmessin, F. Lefèvre and A. Stolzenbach acknowledge support from CNES and from the Programme National de Planétologie (PNP) of CNRS/INSU. C. D. Parkinson also acknowledges support with funding in part by NASA Grant #NNX11AD81G to the University of Michigan. Limaye

acknowledges support for NASA Participating Scientist for Venus Express Grant # NNX09AE85G. The HST observations were obtained through NASA/HST program 12433. Support for this program was provided through a grant from Space Science Telescope Institute, which is operated by the Association of Universities for Research in Astronomy, Inc., under NAS5-26555. Additional funding for the analysis of the HST observations was provided through funding from the NASA Early Careers Program, NASA Grant NNX11AN81G and the NASA Planetary Atmospheres Program, Grant NNX12AG55G. The authors would additionally like to acknowledge Adriana Ocampo, NASA Headquarters, John Grunsfield, NASA Headquarters, Alan Stern, SwRI, Claus Leither, Space Telescope Science Institute, and Håkan Svedhem, Venus Express Project Scientist for their support in the acquisition of the joint HST-Venus Express Venus Observing Campaign.

References

1. Barker, E.S., *Detection of SO_2 in the UV Spectrum of Venus.* Geophys. Res. Lett., 1979. **6**(2): p. 117–120.
2. Conway, R., R. McCoy, C.A. Barth, and A.L. Lane, *IUE detection of sulfur dioxide in the atmosphere of Venus.* Geophys. Res. Lett., 1979. **6**(7): p. 629-631.
3. Stewart, A.I., L.W. Anderson, L. Esposito, and C.A. Barth, *Ultraviolet Spectroscopy of Venus: Initial Results from the Pioneer Venus Orbiter.* Science, 1979. **203**: p. 777-779.
4. Esposito, L.W., M. Copley, R. Eckert, L. Gates, A.I.F. Stewart, and H. Worden *Sulfur Dioxide at the Venus Cloud Tops, 1978–1986.* J. Geophys. Res., 1988. **93**(D5): p. 5267–5276.
5. Na, C.Y., L.W. Esposito, and T.E. Skinner, *International Ultraviolet Explorer Observation of Venus SO2 and SO.* J. Geophys. Res., 1990. **95**(D6): p. 7485–7491.
6. McClintock, W.E., C.A. Barth, and R.A. Kohnert, *Sulfur Dioxide in the Atmosphere of Venus: I. Sounding Rocket Observations.* Icarus, 1994. **112**(2): p. 382-388.
7. Na, C.Y., L. Esposito, W.E. McClintock, and C.A. Barth, *Sulfur Dioxide in the Atmosphere of Venus: II. Modeling Results.* Icarus, 1994. **112**(2): p. 389-395.
8. Na, C.Y. and L. Esposito. *UV Observation of Venus with HST*. in *27th AAS/DPS Annual Meeting, Hawaii, Oct. 9-13*. 1995.
9. Moroz, V.I., D. Spänkuch, D. Titov, K. Schäfer, A. Dyachkov, W. Dohler, L.V. Zasova, D. Oertel, V. Linkin, and J. Nopirakowski, *Water vapor and sulfur dioxide abundances at the Venus cloud tops from the Venera-15 infrared spectrometry data.* Adv. Space Res., 1990. **10**(5): p. 77-81.
10. Zasova, L.V., V. Moroz, L. Esposito, and C.Y. Na, *SO2 in the Middle Atmosphere of Venus: IR Measurements from Venera-15 and Comparison to UV Data.* Icarus, 1993. **105**(1): p. 92-109.
11. Oyama, V., G. Carle, F. Woeller, and J. Pollack, *Venus Lower Atmospheric Composition: Analysis by Gas Chromatography.* Science, 1979. **203**(4382): p. 802-805.
12. Oyama, V., G. Carle, F. Woeller, J.B. Pollack, R. Reynolds, and R. Craig, *Pioneer Venus gas chromatography of the lower atmosphere of Venus.* J. Geophys. Res., 1980. **85**(A13): p. 7891-7902.
13. Gel'man, B., V. Zolotukhin, N. Lamonov, B. Levchuk, A. Lipatov, L. Mukhin, D. Nenarokov, V. Rotin, and B. Okhotnikov, *An analysis of the chemical composition of the atmosphere of Venus on an AMS of the Venera 12 using a gas chromatograph.* Cosmic Res., 1979. **17**: p. 585-589.
14. Hoffman, J., R.R. Hodges Jr., T.M. Donahue, and M.B. McElroy, *Composition of the Venus lower atmosphere from the Pioneer Venus mass spectrometer.* J. Geophys. Res., 1980. **85**(A13): p. 7882-7890.
15. Bertaux, J.L., T. Widemann, A. Hauchecorne, V.I. Moroz, and A.P. Ekonomov, *VEGA 1 and VEGA 2 entry probes: An investigation of local UV absorption (220-400 nm) in the atmosphere of Venus (SO_2, aerosols, cloud structure).* J. Geophys. Res., 1996. **101**(E5): p. 12709-12746.
16. Bézard, B., C. de Bergh, B. Fegley, J.P. Maillard, D. Crisp, T. Owen, J.B. Pollack, and D.H. Grinspoon, *The abundance of sulfur dioxide below the clouds of Venus.* Geophys. Res. Lett., 1993. **20**(15): p. 1587-1590.
17. Pollack, J.B., J.B. Dalton, D.H. Grinspoon, R.B. Wattson, R. Freedman, D. Crisp, D.A. Allen, B. Bézard, C. de Bergh, L.P. Giver, Q. Ma, and R. Tipping, *Near-Infrared Light from Venus' Nightside: A Spectroscopic Analysis.* Icarus, 1993. **103**(1): p. 1-42.

18. Butler, B.J., P.G. Steffes, S.H. Suleiman, M.A. Kolodner, and J.M. Jenkins, *Accurate and Consistent Microwave Observations of Venus and Their Implications.* Icarus, 2001. **154**(2): p. 226-238.
19. Jenkins, J.M., M.A. Kolodner, B.J. Butler, S.H. Suleiman, and P.G. Steffes, *Microwave remote sensing of the temperature and distribution of sulfur compounds in the lower atmosphere of Venus.* Icarus, 2002. **158**: p. 312-328.
20. Arney, G., V. Meadows, D. Crisp, S.J. Schmidt, J. Bailey, and T. Robinson, *Spatially resolved measurements of H_2O, HCl, CO, OCS, SO_2, cloud opacity, and acid concentration in the Venus near-infrared spectral windows.* J. Geophys . Res.: Planets, 2014. **119**(8): p. 1860-1891.
21. Fegley Jr., B., G. Klingelhöfer, K. Lodders, and T. Widemann, *Geochemistry of surface-atmosphere interactions on Venus*, in *Venus II*, S.W. Bougher, D.M. Hunten, and R.J. Phillips, Editors. 1997, The University of Arizona Press: Tucson. p. 591-636.
22. Bullock, M.A. and D.H. Grinspoon, *The Recent Evolution of Climate on Venus.* Icarus, 2001. **150**(1): p. 19-37.
23. Shalygin, E., W. Markiewicz, A. Basilevsky, D.V. Titov, N. Ignatiev, and J.W. Head, *Active volcanism on Venus in the Ganiki Chasma rift zone.* Geophys. Res. Lett., 2015: p. 10.1002/2015GL064088.
24. Smrekar, S.E., E.R. Stofan, N. Mueller, A. Treiman, L. Elkins-Tanton, J. Helbert, G. Piccioni, and P. Drossart, *Recent Hotspot Volcanism on Venus from VIRTIS Emissivity Data.* Science, 2010. **328**: p. 605-07.
25. Esposito, L.W., J.R. Winick, and A.I. Stewart, *Sulfur Dioxide in the Venus Atmosphere: Distribution and Implications.* Geophys. Res. Lett., 1979. **6**(7): p. 601–604.
26. Bertaux, J.L., D. Nevejans, O. Korablev, E. Villard, E. Quémerais, E. Neefs, F. Montmessin, F. Leblanc, J.P. Dubois, E. Dimarellis, A. Hauchecorne, F. Lefevre, P. Rannou, J.Y. Chaufray, M. Cabane, G. Cernogora, G. Souchon, F. Semelina, A. Reberac, E. Van Ransbeek, S. Berkenbosch, R. Clairquin, C. Muller, F. Forget, F. Hourdin, O. Talagrand, A. Rodin, A. Fedorova, A. Stepanov, A. Vinogradov, A. Kiselev, Y. Kalinnikov, G. Durry, B. Sandel, A. Stern, and J.C. Gérard, *SPICAV on Venus Express: Three spectrometers to study the global structure and composition of the Venus atmosphere.* Planet. Space Sci., 2007. **55**(12): p. 1673-1700.
27. Belyaev, D., F. Montmessin, J.L. Bertaux, A. Mahieux, A. Fedorova, O. Korablev, E. Marcq, Y. Yung, and X. Zhang, *Vertical profiling of SO2 and SO above Venus' clouds by SPICAV/SOIR solar occultations.* Icarus, 2012. **217**(2): p. 740-751.
28. Belyaev, D., O. Korablev, A. Fedorova, J.L. Bertaux, A.C. Vandaele, F. Montmessin, A. Mahieux, V. Wilquet, and R. Drummond, *First observations of SO2 above Venus' clouds by means of solar occultation in the infrared.* J. Geophys. Res., 2008. **113**: p. doi:10.1029/2008JE003143.
29. Mahieux, A., A.C. Vandaele, S. Robert, V. Wilquet, R. Drummond, D. Belyaev, and J.L. Bertaux, *Venus mesospheric sulfur dioxide measurement retrieved from SOIR on board Venus Express.* Planet. Space Sci., 2015. **113-114**: p. 193-204.
30. Marcq, E., B. Bézard, P. Drossart, G. Piccioni, J.M. Reess, and F. Henry, *A latitudinal survey of CO, OCS, H_2O, and SO_2 in the lower atmosphere of Venus: Spectroscopic studies using VIRTIS-H.* J. Geophys. Res., 2008. **113**(E00B07): p. doi:10.1029/2008JE003074.
31. Jessup, K.L., E. Marcq, F. Mills, A. Mahieux, S. Limaye, C. Wilson, M. Allen, J.-L. Bertaux, W. Markiewicz, T. Roman, A.C. Vandaele, V. Wilquet, and Y. Yung, *Coordinated Hubble Space Telescope and Venus Express Observations of Venus' upper cloud deck.* Icarus, 2015. **258**: p. 309–336.

32. Encrenaz, P., T. Greathouse, H. Roe, M. Richter, J. Lacy, B. Bézard, T. Fouchet, and T. Widemann, *HDO and SO_2 thermal mapping on Venus: evidence for strong SO_2 variability.* Astron. Astrophys., 2012. **543**: p. 10.1051/0004-6361/201219419.
33. Sandor, B.J., R.T. Clancy, G. Moriarty-Schieven, and F.P. Mills, *Sulfur Chemistry in the Venus Mesosphere from SO_2 and SO Microwave Spectra.* Icarus, 2010. **208**(1): p. 49-60.
34. Encrenaz, T., R. Moreno, A. Moullet, E. Lellouch, and T. Fouchet, *Submillimeter mapping of mesospheric minor species on Venus with ALMA.* Planet. Space Sci., 2015. **113**: p. 275-291.
35. Krasnopolsky, V., *Spatially-resolved high-resolution spectroscopy of Venus 2. Variations of HDO, OCS, and SO_2 at the cloud tops.* Icarus, 2010. **209**(2): p. 314-322.
36. Marcq, E., D. Belyaev, F. Montmessin, A. Fedorova, J.L. Bertaux, A.C. Vandaele, and E. Neefs, *An investigation of the SO_2 content of the venusian mesosphere using SPICAV-UV in nadir mode.* Icarus, 2011. **211**: p. 58–69.
37. Marcq, E., J.L. Bertaux, F. Montmessin, and D. Belyaev, *Variations of sulphur dioxide at the cloud top of Venus's dynamic atmosphere.* Nature Geoscience, 2013. **6**: p. 25-28.
38. Encrenaz, T., T. Greathouse, M. Richter, J. Lacy, T. Widemann, B. Bézard, T. Fouchet, C. de Witt, and S. Atreya, *HDO and SO_2 thermal mapping on Venus. II. The SO_2 spatial distribution above and within the clouds.* Astron. Astrophys., 2013. **559**(A65): p. DOI: 10.1051/0004-6361/201322264.
39. Nevejans, D., E. Neefs, E. Van Ransbeeck, S. Berkenbosch, R. Clairquin, L. De Vos, W. Moelans, S. Glorieux, A. Baeke, O. Korablev, I. Vinogradov, Y. Kalinnikov, B. Bach, J.P. Dubois, and E. Villard, *Compact high-resolution space-borne echelle grating spectrometer with AOTF based on order sorting for the infrared domain from 2.2 to 4.3 micrometer.* Applied Optics, 2006. **45**(21): p. 5191-5206.
40. Mahieux, A., V. Wilquet, R. Drummond, D. Belyaev, A. Fedorova, and A.C. Vandaele, *A New Method for Determining the transfer function of an Acousto Optical Tunable Filter.* Optics Express, 2009. **17**: p. 2005-2014.
41. Mahieux, A., *Inversion of the infrared spectra recorded by the SOIR instrument on board Venus Express*. 2011, Thesis, Univ. Libre de Bruxelles, Belgium.
42. Vandaele, A.C., A. Mahieux, S. Robert, R. Drummond, V. Wilquet, and J.L. Bertaux, *Carbon monoxide short term variability observed on Venus with SOIR/VEX.* Planet. Space Sci., 2015. **113-114**: p. 237-255.
43. Mahieux, A., A.C. Vandaele, S.W. Bougher, R. Drummond, S. Robert, V. Wilquet, A. Piccialli, F. Montmessin, S. Tellmann, M. Pätzold, B. Häusler, and J.L. Bertaux, *Update of the Venus density and temperature profiles at high altitude measured by SOIR on board Venus Express.* Planet. Space Sci., 2015. **113-114**: p. 309-320.
44. Mahieux, A., A.C. Vandaele, S. Robert, V. Wilquet, R. Drummond, F. Montmessin, and J.L. Bertaux, *Densities and temperatures in the Venus mesosphere and lower thermosphere retrieved from SOIR on board Venus Express: Carbon dioxide measurements at the Venus terminator.* J. Geophys. Res., 2012. **117**(E07001): p. doi:10.1029/2012JE004058.
45. Bertaux, J.L., O. Korablev, S. Perrier, E. Quémerais, F. Montmessin, F. Leblanc, S. Lebonnois, P. Rannou, F. Lefèvre, F. Forget, A. Fedorova, E. Dimarellis, A. Reberac, D. Fonteyn, J.Y. Chaufray, and S. Guibert, *SPICAM on Mars Express: Observing modes and overview of UV spectrometer data and scientific results.* J. Geophys. Res., 2006. **111**(E10S90).
46. Piccialli, A., F. Montmessin, D. Belyaev, A. Mahieux, A. Fedorova, E. Marcq, J.L. Bertaux, A.C. Vandaele, and O. Korablev, *Thermal structure of Venus upper*

aymosphere measured by stellar occultations with SPICAV/Venus Express. Planet. Space Sci., 2015. **113-114**: p. 321-335.
47. Montmessin, F., J.L. Bertaux, F. Lefèvre, E. Marcq, D. Belyaev, J.C. Gérard, O. Korablev, A. Fedorova, V. Sarago, and A.C. Vandaele, *A layer of ozone detected in the nightside upper atmosphere of Venus.* Icarus, 2011. **216**: p. 82-85.
48. Marcq, E., B. Bézard, T. Encrenaz, and M. Birlan, *Latitudinal variations of CO and OCS in the lower atmosphere of Venus from near-infrared nightside spectro-imaging.* Icarus, 2005. **179**(2): p. 375-386.
49. Marcq, E., T. Encrenaz, B. Bézard, and M. Birlan, *Remote sensing of Venus' lower atmosphere from ground-based IR spectroscopy: Latitudinal and vertical distribution of minor species.* Planet. Space Sci., 2006. **54**(13-14): p. 1360-1370.
50. Matthews, H.E., *The James Clerk Maxwell Telescope: A Guide for the Prospective User, available on www.jach.hawaii.edu*, H. Joint Astronomy Centre, Hawaii, Editor. 2003.
51. Clancy, R.T., B. Sandor, and G. Moriarty-Schieven, *Thermal structure and CO distribution for the Venus mesosphere/lower thermosphere: 2001–2009 inferior conjunction sub-millimeter CO absorption line observations.* Icarus, 2012. **217**(2): p. 779-793.
52. Esposito, L.W., J.L. Bertaux, V. Krasnopolsky, V.I. Moroz, and L.V. Zasova, *Chemistry of lower atmosphere and clouds*, in *Venus II: Geology, Geophysics, Atmosphere, and Solar Wind Environment*, S.W. Bougher, D.M. Hunten, and R.J. Phillips, Editors. 1997, Univ. of Arizona Press. p. 415-458.
53. Sandor, B., R.T. Clancy, and G. Moriarty-Schieven, *Upper limits for H_2SO_4 in the mesosphere of Venus.* Icarus, 2012. **217**(2): p. 839-844.
54. Clancy, R.T., B. Sandor, and G. Moriarty-Schieven, *Venus Upper Atmospheric CO, Temperature, and Winds across the Afternoon/Evening Terminator from June 2007 JCMT Sub-millimeter Line Observations.* Planet. Space Sci., 2008. **56**(10): p. 1344-1354.
55. Belyaev, D., D. Evdokimova, F. Montmessin, E. Marcq, A. Fedorova, O. Korablev, J.L. Bertaux, and M. Luginin, *Night side distribution of SO_2 content in Venus' upper mesosphere.* Icarus, 2016. **(subm.)**.
56. Belyaev, D., D. Evdokimova, F. Montmessin, E. Marcq, A. Fedorova, O. Korablev, and J.L. Bertaux. *Distribution of SO_2 content at the night side of Venus' upper mesosphere*. in *International Venus Conference*. 2016. Oxford, UK, 4-8 April.
57. Krasnopolsky, V.A., *Vertical profile of H2SO4 vapor at 70–110 km on Venus and some related problems.* Icarus, 2011. **215**: p. 197-203.
58. Hedin, A.E., H.B. Niemann, and W.T. Kasprzak, *Global empirical model of the Venus thermosphere.* J. Geophys. Res., 1983. **88**(A1): p. 73-83.
59. Zasova, L.V., V.I. Moroz, V.M. Linkin, I.A. Khatountsev, and B.S. Maiorov, *Structure of the Venusian Atmosphere from Surface up to 100 km.* Cosmic Res., 2006. **44**(4): p. 364-383.
60. Krasnopolsky, V.A., *A photochemical Model for the Venus Atmosphere at 47-112 km.* Icarus, 2012. **218**(1): p. 230-246.
61. Mills, F.P. and M. Allen, *A review of selected issues concerning the chemistry in Venus' middle atmosphere.* Planet. Space Sci., 2007. **55**(12): p. 1729-1740.
62. Zhang, X., M. Liang, F. Mills, D. Belyaev, and Y. Yung, *Sulfur chemistry in the middle atmosphere of Venus.* Icarus, 2012. **217**(2): p. 714-739.
63. Parkinson, C., P. Gao, R. Schulte, S.W. Bougher, Y. Yung, C.G. Bardeen, V. Wilquet, A.C. Vandaele , A. Mahieux, S. Tellmann, and M. Patzold, *Distribution of Sulphuric*

Acid Aerosols in the Clouds and Upper Haze of Venus Using Venus Express VAST and VeRa Temperature Profiles. Planet. Space Sci., 2015. **113-114**: p. 205-218.
64. Stolzenbach, A., F. Lefèvre, S. Lebonnois, A. Määttänen, and S. Bekki. *Three-dimensional modelling of Venus photochemistry*. in *EGU General Assembly*. 2014. Vienna, Austria.
65. Mills, F.P., L.W. Esposito, and Y.L. Yung, *Atmospheric composition, chemistry and clouds.* Geophysical Monograph Series, 2007. **176**: p. 73-100.
66. Zhang, X., M.C. Liang, F. Montmessin, J.L. Bertaux, C. Parkinson, and Y.L. Yung, *Photolysis of sulphuric acid as the source of sulphur oxides in the mesosphere of Venus.* Nature Geoscience, 2010. **3**: p. 834-7.
67. Parkinson, C., P. Gao, L. Esposito, Y. Yung, S.W. Bougher, and M. Hirtzig, *Photochemical control of the distribution of Venusian water.* Planet. Space Sci., 2015. **113-114**: p. 226-236.
68. Krasnopolsky, V., *S_3 and S_4 abundances and improved chemical kinetic model for the lower atmosphere of Venus.* Icarus, 2013. **225**(1): p. 570-580.
69. Krasnopolsky, V., *Nighttime photochemical model and night airglow on Venus.* Planet. Space Sci., 2013. **85**: p. 78.
70. Irwin, P.G.J., K. de Kok, A. Negrao, C. Tsnag, C.F. Wilson, P. Drossart, G. Piccioni, D. Grassi, and F.W. Taylor, *Spatial variability of carbon monoxide in Venus' mesosphere from Venus Express/VIRTIS measurements.* J. Geophys. Res., 2008. **113**(E00B01): p. 10.1029/2008JE003093.
71. Tellmann, S., M. Pätzold, B. Häusler, M.K. Bird, and G.L. Tyler, *Structure of the Venus neutral atmosphere as observed by the Radio Science experiment VeRa on Venus Express.* J. Geophys. Res., 2009. **114**(E0B36).
72. Haus, R., D. Kappel, and G. Arnold, *Atmospheric thermal structure and cloud features in the southern hemisphere of Venus as retrieved from VIRTIS/VEX radiation measurements.* Icarus, 2014. **232**: p. 232-248.
73. Ayers, G.P., R.W. Gillett, and J. Gras, *On the vapor pressure of sulfuric acid.* Geophys. Res. Lett., 1980. **7**: p. 433-436.
74. Kulmala, M. and A. Laaksonen, *Binary nucleation of water‐ sulphuric acid system: Comparison of classical theories with different H2SO4 saturation vapour pressures.* J. Chem. Phys., 1990. **93**: p. 696-701.
75. Richardson, C., R. Hightower, and A. Pigg, *Optical measurement of the evaporation of sulfuric acid droplets.* Applied Optics, 1986. **25**: p. 1226-1229.
76. Stull, D., *Vapor pressure of pure substances—Inorganic compounds.* Ind. Eng. Chem., 1947. **39**: p. 540-550.
77. Burkholder, J.B., M. Mills, and S. McKeen, *Upper limit for the UV absorption cross sections of H_2SO_4.* Geophys. Res. Lett., 2000. **27**: p. 2493-2496.
78. Hintze, P., H.G. Kjaergaard, V. Vaida, and J.B. Burkholder, *Vibrational and electronic spectroscopy of sulfuric acid vapor.* J. Phys. Chem., 2003. **A 107**: p. 1112-1118.
79. Sandor, B., R.T. Clancy, and G. Moriarty-Schieven. *SO and SO2 in the Venus Meso-sphere: Observations of Extreme and Rapid Variation.* . in *Bull. Amer. Astron. Soc.* 2007.
80. Petrass, J.B., *Modelling of sulfur oxide and cloud chemistry in Venus' mesosphere*. 2013, The Australian National University. p. 66.